AD-A106 286 AIR FORCE INST OF TECH WRIGHT-PATTERSON AFB OH F/G 20/4
FINITE ELEMENT METHOD IN TRANSIENT AERODELASTIC PROBLEM.(U)
1979 H C BRIGGS
UNCLASSIFIED AFIT-CI-79-256D NL

LEVEL II

UNCLASS

SECURITY CLASSIFICATION OF THIS PAGE (When Data Entered)

REPORT DOCUMENTATION PAGE

READ INSTRUCTIONS BEFORE COMPLETING FORM

1. REPORT NUMBER: 79-256D	2. GOVT ACCESSION NO.: AD-A106286
3. RECIPIENT'S CATALOG NUMBER:	
4. TITLE (and Subtitle): Finite Element Method in Transient Aeroelastic Problems	5. TYPE OF REPORT & PERIOD COVERED: THESIS/DISSERTATION
	6. PERFORMING ORG. REPORT NUMBER:
7. AUTHOR(s): Captain Hugh Clark Briggs	8. CONTRACT OR GRANT NUMBER(s):
9. PERFORMING ORGANIZATION NAME AND ADDRESS: AFIT STUDENT AT: Columbia University	10. PROGRAM ELEMENT, PROJECT, TASK AREA & WORK UNIT NUMBERS:
11. CONTROLLING OFFICE NAME AND ADDRESS: AFIT/NR, WPAFB OH 45433	12. REPORT DATE: 1979
	13. NUMBER OF PAGES: 102
14. MONITORING AGENCY NAME & ADDRESS (if different from Controlling Office)	15. SECURITY CLASS. (of this report): UNCLASS
	15a. DECLASSIFICATION/DOWNGRADING SCHEDULE:

16. DISTRIBUTION STATEMENT (of this Report)

APPROVED FOR PUBLIC RELEASE; DISTRIBUTION UNLIMITED

DTIC ELECTE OCT 29 1981 E

17. DISTRIBUTION STATEMENT (of the abstract entered in Block 20, if different from Report)

20 OCT 1981

18. SUPPLEMENTARY NOTES

APPROVED FOR PUBLIC RELEASE: IAW AFR 190-17

FREDRIC C. LYNCH, Major, USAF
Director of Public Affairs
Air Force Institute of Technology (ATC)
Wright-Patterson AFB, OH 45433

19. KEY WORDS (Continue on reverse side if necessary and identify by block number)

20. ABSTRACT (Continue on reverse side if necessary and identify by block number)

ATTACHED

81 10 26 165

DD FORM 1 JAN 73 1473 EDITION OF 1 NOV 65 IS OBSOLETE UNCLASS

AD A106286

DTIC FILE COPY

79-256D

AUTHOR: Hugh Clark Briggs

TITLE: Finite Element Method in Transient Aeroelastic Problems

RANK: Captain

SERVICE: Air Force

YEAR: 1979

PAGES: 102

DEGREE: Doctor of Engineering Science

INSTITUTION: Columbia University

ACKNOWLEDGMENT

I wish to express my sincere gratitude to Dr. M. P. Bieniek for his invaluable instruction and attention over the past two years and to Dr. R. Skalak for his suggestions and guidance. In addition, I thank Mrs. Reva Goldkopf for her energetic typing of the manuscript. My appreciation also goes to my wife, Brenda, who was always encouraging and understanding.

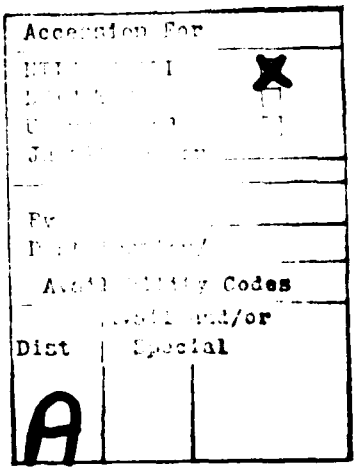

ABSTRACT

This dissertation presents the development of a finite element method of analysis of interaction problems between an elastic structure and a moving fluid. The fundamental principles of the method have been formulated for the case of finite non-isothermal deformations of the structure and unsteady flow of a compressible, viscous, heat-conducting fluid. Details of the method and numerical examples have been worked out for the simpler, and yet practically important conditions of isothermal deformations of the structure and compressible, inviscid, isentropic flow of the fluid.

The finite element formulation of the method represents a numerical solution of the variational equations of the problem. The necessary variational principles have been derived for the fluid, for the structure, and for the joint fluid-structure system. Since the governing equations of the fluid do not form a potential operator, the corresponding variational functional has been constructed in terms of the actual and adjoint variables. Similar variational functionals have been obtained for the structure and for the iteraction problem. Consequently, the resulting finite element algorithm belongs to the class of "weighted residuals" methods.

A quadrilateral isoparametric element has been developed and used for the fluid. In order to remove

the instability effects inherent to the problems with convective terms, the "upwind weighting" procedure has been employed. The structure can, conceivably, be represented by any type of elements; in the present examples, a compatible membrane element has been used.

The numerical examples demonstrate, first, the application of the method for the analysis of transient problems of gas dynamics in one and two dimensions. Subsequently, transient motion of a membrane interacting with a two-dimensional gas flow, and the resulting perturbations in the gas itself, have been analyzed.

TABLE OF CONTENTS

1. INTRODUCTION

The goal of the present method is to analyze fluid structure interactions of a general nature. The structure is an elastic solid of arbitrary configuration. The fluid is modeled as a compressible linear Newtonian fluid. The method is not restricted to small displacements in the structure, nor small perturbations in the fluid.

The equations of motion, conservation of mass, and conservation of energy form the basis for the method. The variational principle is stated in general coordinates but most work is in Cartesian coordinates. This change is for convenience only and does not represent a limitation of the method. The structural equations allow large displacements and thermal strains. The fluid is formulated in spatial coordinates, and the resulting convected gradients are included. The fluid is not restricted to being at rest initially.

The problem solution is based upon the finite element method for both fluid and structure. Contributions have been made to the use of upwind weighting to stabilize the numerical solution of the fluid dynamics equations. The ability of finite elements to approximate complex shapes allows the analysis of very general configurations. Further, the extremely simple handling

of the fluid structure interface is a major reason for the success of the numerical application of the method.

To demonstrate the viability of the method, several numerical examples are presented. The Newtonian fluid model is reduced to an ideal gas to simplify the numerical procedure. As a result, the interface boundary condition is reduced to full slip or continuity of the surface normal velocity. The examples include one-dimensional gas dynamics and vibration of an elastic membrane.

The finite element method is instrumental in the effective solution of the arbitrary problems at hand. The present method will allow the use of virtually any structural element in current program libraries, thereby allowing the extension of previous problems to include interaction effects. Although the numerical examples of this work are problems of unsteady motion, the functional and the discretization process are directly applicable to other problem types. Some caution is indicated, however, as the equations of the problem are nonlinear differential equations. Despite the limited success of the present work, much remains to be done in the numerical solution of problems of this nature.

By far the most common formulation of structural finite elements is based upon the displacements and velocities. In contrast, fluid dynamics problems are more

frequently based upon the velocity potential or the stream function and vorticity. As examples of fluid structure interaction become more common, a shift to the use of velocity has occurred. The use of a common basis for both structure and fluid as is done here can simplify the mechanization of many aspects of the problem solution.

The handling of the interface in the present work is simplified greatly by treating this region much as a structural method handles an inhomogeneous medium. That is, as long as the velocity field is continuous across the surface, no other conditions need be explicitly represented. When using finite elements in practice, this means using compatible elements on the interface. Further, it requires coincidence of the structural and fluid nodes. As a result, the common difficulties arising from differing mesh densities do not occur.

A result of the present work is the demonstration by numerical examples of a new unified method for fluid structure interaction problems. The method is unified in the sense that the entire problem domain is formulated and solved by the same procedure. Differences in treatment of the structure and fluid domains arise as a result of numerical stability requirements rather than the variational formulation.

2. BACKGROUND

There appears to be no published examples of fluid structure interaction involving a compressible viscous fluid in unsteady motion. It seems little attention has been paid to formulating the solution procedure for such a fluid until recently (Nakamura, 1977 and Chung, 1978). By far the most developed fluid solution procedures are for potential flow, acoustic fluids, and creeping viscous flow. Whatever the reason for this, it is probably not unrelated to the fact that these three classes of fluid problems have simple variational formulations. Due to the well established position of these procedures, they are the dominant formulations employed in interaction problems.

For example, some of the specific fluid structure combinations that have been tried are: elastic shells and acoustic fluid, both by finite differences (DiMaggio, Bleich, McCormick, 1978); elasto-plastic shells and acoustic fluid, again by finite differences (Nikolakopoulou, DiMaggio, 1978); elastic beams with acoustic fluid by finite elements (Zarda, 1976); elastic bodies and incompressible viscous fluids by finite elements (Zarda, Chien, Skalak, 1977); elastic structural response to internal explosion with an acoustic fluid (Jacobson, Yamane, Brues, 1977).

In addition, a lot of work has been done to

uncouple the problem by employing a suitable approximation for the fluid response. Two of the most common are the doubly asymptotic approximation and supersonic thin airfoil theory. Examples of the former are: elastic structural response to shock (Ranlet, DiMaggio, Bleich, Baron, 1977); elasto-plastic structural response to shock (Atkatsh, Baron, Bieniek, 1978); elastic structural response (Everstine, 1976 and Everstine, Schroeder, Marcus, 1975); transient structural response (Geers, 1975).

The use of supersonic thin airfoil theory allows the local pressure to be related to the structural slope and velocity. Examples are: elastic panel stability (Kornecki, Dowell, O'Brien, 1976); panel flutter (Olson, 1970 and Dowell, 1970); large deflection plate flutter (Dowell, 1966); Lyapunov stability analysis of panels (Wang, 1966); stability of cylindrical shell limit cycle oscillations (Evensen, Olson, 1968).

Several other fluid solution procedures are commonly used in iterative solution processes. By separating the problem at each iteration, the method used to calculate the fluid response is almost entirely divorced from the structural solution method. For this reason fluid solution techniques will be considered independently from the structural method in the following.

Perhaps the fastest growing inviscid procedure is the doublet lattice method, although other methods of

singularity distribution are also used. Some are: doublet lattice method for interfering wings and bodies (Rodden, Giesing, Kalman, 1970 and Giesing, Kalman, Rodden, 1972); vortex lattice for lifting surfaces (Pittman, Dillon, 1977); doublet lattice (Jordan, 1978); distributed sources and doublets in a paneling method (Dusto, Epton, Johnson, 1978); distributed sources for bluff body wakes (Parkinson, Jandali, 1970); distributed doublets with cubic spline interpolation functions (Gotta, van de Vooren, 1972).

One other method is finding acceptance for certain linear inviscid problems. Known variously as the Green's function method or the boundary solution procedure, its chief advantage is to reduce volume problems to surface problems. The former has been applied to potential flow where the surface is modeled by flat quadrilaterals (Morino, 1973). The latter has been used in surface wave problems (Zienkiewicz, 1977) and other problems (Zienkiewicz, Kelly, Bettes, 1977).

For viscous fluids, the majority of the work has been done in very low Reynolds number flows. Here a simple variational principle leads to minimizing the dissipation. Some examples are: Newtonian and special non-Newtonian fluids (Delleur, Sooky, 1961); Galerkin's method with the use of Lagrangian multiplier for incompressibility (Argyris, Mareczek, 1974);

minimization of dissipation with finite elements (Oden, Somogoyi, 1969). Alternate formulations for viscous flows include the stream function and vorticity (Baker, 1974 and Tuann, Olson, 1976). Series solutions have been applied, for example, to elastic spheres in close fitting tubes (Tözeren, Skalak, 1978).

When studying higher Reynolds number flow, the use of upwind differencing (Steele, Barrett, 1978) or upwind weighting (Christie, Griffiths, Mitchel, Zienkiewicz, 1976) brings numerical stability. This technique is being mentioned more frequently in new texts (Chung, 1978) but few numerical examples beyond two-dimensional temperature convection (Zienkiewicz, 1977) are given.

3. VARIATIONAL FORMULATION OF THE PROBLEM

3.1 Existing Variational Principles

Examination of the variational methods of fluid dynamics reveals that there is no established common variational principle valid for compressible viscous fluids in unsteady motion. In fact, Finlayson (1972) has shown that the Navier Stokes equations do not comprise a potential operator. Thus, there is no variational principle in the conventional sense.

In the context of the present search for a general procedure, the existing variational principles suffer from one of two difficulties. Most frequently, the problem must be restricted or simplified to obtain a functional. An example is the assumption of small velocities and incompressibility in creeping viscous flow. Secondly, side conditions may be imposed on the trial functions. As the problems become more complex, it is difficult to include all the equations in the functional without introducing unknown multipliers. Such conditions are then left as constraints on the trial functions and can complicate the numerical solution procedure.

For inviscid compressible flow of a perfect gas, Serrin (1959) presents a functional based primarily on kinetic and internal energies. The continuity equation

and the isentropic condition are added by using multipliers. This leads to a formulation based upon velocity, density, entropy and two multipliers. A later modification, attributed to C.C. Lin by Finlayson, includes the material coordinates and a multiplier to insure that these coordinates do not change in rotational flow.

The most common inviscid principles are based upon the velocity potential. For steady incompressible flow the equation to be solved is Laplace's equation in the velocity potential. The well-known functional involves the sum of the squares of the spatial gradients of the potential.

A functional for steady compressible isentropic flow based upon the velocity potential is easily constructed (Carey, 1975 and Norrie, de Vries, 1973). The functional is

$$I(\phi) = \int_V \frac{1}{2} \int_0^{t=(\phi_{,i})^2} \rho(t)\,dt\,dV \qquad (3.1\text{-}1)$$

where

$$\rho(t) = \left[1 + \frac{\gamma - 1}{2} M_\infty^2 (1 - t)\right]^{\frac{1}{\gamma - 1}} \qquad (3.1\text{-}2)$$

The Euler equation for this functional is the steady continuity equation in terms of the potential ϕ,

$$(\rho\phi_{,i})_{,i} = 0 \qquad (3.1\text{-}3)$$

Carey (1975) suggests the solution should be based upon discretization by finite elements followed by a perturbation expansion to handle the required root. The first term in such an expansion leads to the incompressible flow equation, and successive terms give compressibility corrections.

A quasi-variational principle for the compressible flow velocity potential equation has been given by Norrie and de Vries (1973). For two-dimensional flow the equation is

$$(\phi_{,x}^2 - a^2)\,\phi_{,xx} + 2\phi_{,x}\phi_{,y}\phi_{,xy} + (\phi_{,y}^2 - a^2)\,\phi_{,yy} = 0 \tag{3.1-4}$$

where the local speed of sound,

$$a = a_\infty^2 + \frac{\gamma - 1}{2} q_\infty^2 + \frac{1 - \gamma}{2} (\phi_{,x}^2 + \phi_{,y}^2) \tag{3.1-5}$$

The functional is written as

$$I(\nu) = \int_V \left[\frac{1}{12a} (\nu_{,x}^4 + \nu_{,y}^4) - \frac{1}{2} (\nu_{,x}^2 + \nu_{,y}^2) + \frac{G}{a^2} (\nu_{,x}\nu_{,y})\right] dV$$
$$- \int_S \left[H\nu + Q\nu + \frac{1}{2} \alpha\nu^2\right] dS \tag{3.1-6}$$

where

$$G = \phi_{,x}\phi_{,y}; \qquad H = \frac{1}{3a^2} (\phi_{,x}^3 n_x + \phi_{,y}^3 n_y) + \frac{G}{a^2} (\phi_{,x} n_y + \phi_{,y} n_x) \tag{3.1-7}$$

The functional of Eq. 3.1-6 has as its Euler equation the preceding differential equation if variations are

permitted in ν only and, after variations, ν is set equal to ϕ. In practice, the functions, G, H and a are evaluated at a previous iteration and treated as known on the next iteration.

For slow viscous incompressible flow the functional has been given by Zarda, Chien and Skalak (1977). The incompressibility condition is included by using the pressure as a multiplier. The functional is

$$I(v_\alpha, p) = \int_V [2\mu d_{\alpha\beta} d_{\alpha\beta} - p v_{\alpha,\alpha}] \, dV + \int_{S_2} v_\alpha \hat{t}_\alpha dS \qquad (3.1\text{-}8)$$

where

$$d_{\alpha\beta} = \frac{1}{2} (v_{\alpha,\beta} + v_{\beta,\alpha}), \qquad (3.1\text{-}9)$$

velocity is specified on S_1 and $\hat{t}_\alpha$ is a prescribed traction on S_2. The Euler equation is

$$2\mu d_{\alpha\beta,\beta} - p_{,\alpha} = 0 \qquad (3.1\text{-}10)$$

while the boundary condition on S_2 is

$$2\mu d_{\alpha\beta} n_\beta - p n_\alpha = \hat{t}_\alpha \qquad (3.1\text{-}11)$$

Steady heat conduction with constant thermal conductivity has a variational principle very similar to incompressible potential flow. The functional is

$$I(T) = \int_V [k T_{,a} T_{,a} - Tr] \, dV + \int_{S_2} T \hat{q}_a n_a dS \qquad (3.1\text{-}12)$$

where $\hat{q}_a$ is a prescribed heat flux on surface S_2, r is the rate of heat generation and T is prescribed on S_1.

The Euler equation is

$$kT_{,aa} + r = 0 \qquad (3.1\text{-}13)$$

and the boundary condition on S_2 is

$$- kT_{,a}n_a = \hat{q}_a n_a \qquad (3.1\text{-}14)$$

The unsteady heat conduction equation is non-selfadjoint due to the presence of the first time derivative. As a result the operator is not potential and no variational principle exists. With certain restrictions, however, the equation can be transformed into a symmetric form. For linear thermoelasticity, for example, the Laplace transform in time can be used to render the equations symmetric (Nickell, Sackman, 1968). The method has the advantage of having the initial conditions contained explicitly in the functional.

The discussion of variational principles would not be complete without a brief mention of the Principle of Minimum Total Potential Energy. The principle is applicable to isothermal motion of an elastic solid. It states that minimizing the sum of the strain energy and the potential of external forces is equivalent to satisfying the equations of motion. Use of the principle requires the specification of the strain energy function. For isotropic materials with nonlinear constitutive equations, a suitable form that will

approximate the behavior of the material can usually be found by using functions of the strain invariants.

3.2 General Method of Construction of Variational Functionals

Several of the more well developed areas of structural and fluid dynamics have in common the existence of functionals and variational principles. Linear elasticity, heat conduction in solids, slow viscous flow and potential flow are just a few of the areas. In most cases, determination of the existence of the functional for a given differential operator has been a matter of trial and error. If the operator represents the Euler equations of a functional, that operator is the gradient of the functional in a variational sense. The operator is then said to be potential. Finlayson (1972) presents a method based upon Fréchet differentials to easily determine whether an operator is potential. He uses the method to demonstrate that a functional does not exist for steady motion of an incompressible viscous fluid unless

$$\underset{\sim}{v} \times (\nabla \times \underset{\sim}{v}) = 0 \quad \text{or} \quad \underset{\sim}{v} \cdot \nabla \underset{\sim}{v} = 0 \qquad (3.2\text{-}1)$$

where $\underset{\sim}{v}$ is the velocity. The following is a summary of Finlayson's work leading to the use of adjoint variables to construct a functional for non-potential operators.

The Fréchet differential of an operator N(u) in the direction ϕ is defined as

$$N_u'\phi = \lim_{\varepsilon \to 0} \frac{N(u+\varepsilon\phi) - N(u)}{\varepsilon} = \left[\frac{\partial}{\partial \varepsilon} N(u+\varepsilon\phi)\right]_{\varepsilon = 0} \tag{3.2-2}$$

The operator N(u) is the gradient of a functional if the Fréchet differential N_u' is symmetric, i.e.,

$$\int \psi N_u'\phi dV = \int \phi N_u'\psi dV \tag{3.2-3}$$

For a potential operator N(u), the functional can be constructed by

$$F(u) = \int u \int_0^1 N(\lambda u) d\lambda dV \tag{3.2-4}$$

For the nonsymmetric operator, N, the definition of the "adjoint" operator, N^*, is

$$N^*(u,u^*) = \tilde{N}_u'u^* \tag{3.2-5}$$

where $\tilde{N}_u'$ is obtained by integration by parts, such that,

$$\int u^* N_u' u dV = \int u \tilde{N}_u' u^* dV + \text{boundary terms} \tag{3.2-6}$$

The functional for the operator N(u) and its adjoint $N^*(u,u^*)$ is

$$I(u,u^*) = \int [u^* N(u) - ug - u^* f]\, dV \tag{3.2-7}$$

The Euler equations are

$$\delta u^{*}: N(u) - f = 0 \tag{3.2-8a}$$

$$\delta u : \tilde{N}'_{u} u^{*} - g = N^{*}(u,u^{*}) - g = 0 \tag{3.2-8b}$$

Thus, if the problem is expanded to include the adjoint equation, a variational principle exists.

3.3 Compressible Newtonian Fluid

Constitutive Relations

The stresses at a point, $P_{\alpha\beta}$, consist of a pressure, p, and viscous stresses, $t_{\alpha\beta}$, such that

$$P_{\alpha\beta} = - p\delta_{\alpha\beta} + t_{\alpha\beta} \tag{3.3-1}$$

The Newtonian fluid model for the viscous stresses assumes

$$t_{\alpha\beta} = \lambda v_{\gamma,\gamma}\delta_{\alpha\beta} + 2\mu d_{\alpha\beta} \tag{3.3-2}$$

where λ and μ are coefficients of viscosity, v_{α} is the velocity and the rate of strain tensor is

$$d_{\alpha\beta} = \frac{1}{2}\,(v_{\alpha,\beta} + v_{\beta,\alpha}) \tag{3.3-3}$$

The equation of state for the pressure can be written as

$$p = \rho RT \tag{3.3-4}$$

For a perfect gas, the entropy function per unit mass is

$$S = \frac{R}{\gamma - 1} \log \frac{p}{\rho^{\gamma}} \tag{3.3-5}$$

and the internal energy, per unit mass,

$$E = C_{v}T \tag{3.3-6}$$

If C_p is the specific heat at constant pressure, and C_v is the specific heat at constant volume, R and γ are defined as

$$R = C_p - C_v$$

$$\gamma = C_p/C_v$$

The heat conduction law is assumed as

$$q_\alpha = - kT,_\alpha \qquad (3.3\text{-}7)$$

where q_α is the heat flux vector, k is the thermal conductivity and T is temperature.

The Governing Differential Equations

The equation of motion for the fluid in spatial coordinates is assumed in the form

$$\rho \frac{Dv_\alpha}{Dt} - P_{\alpha\beta,\beta} - \rho f_\alpha = 0 \qquad (3.3\text{-}8)$$

where f_α is the body force vector per unit mass. After using the Newtonian fluid model and the perfect gas law, the equation of motion becomes

$$\rho \frac{Dv_\alpha}{Dt} - \lambda v_{\beta,\beta\alpha} - 2\mu d_{\alpha\beta,\beta} + (RT\rho),_\alpha - \rho f_\alpha = 0 \qquad (3.3\text{-}9)$$

The equation of continuity or conservation of mass is

$$\frac{D\rho}{Dt} + \rho v_{\alpha,\alpha} = 0 \qquad (3.3\text{-}10)$$

The energy equation is

$$\rho\left(\frac{DE}{Dt} + \frac{1}{2}\frac{Dv_\alpha^2}{Dt}\right) = (P_{\alpha\beta}v_\alpha)_{,\beta} - q_{\alpha,\alpha} + \rho f_\alpha v_\alpha \qquad (3.3\text{-}11)$$

Dotting the equation of motion into the velocity and subtracting gives the thermodynamic energy equation,

$$\rho\frac{DE}{Dt} = P_{\alpha\beta}v_{\alpha,\beta} - q_{\alpha,\alpha} \qquad (3.3\text{-}12)$$

After inserting the Newtonian fluid model, the perfect gas law, and the heat conduction law, the result is the temperature equation,

$$C_v\frac{DT}{Dt} + RTv_{\alpha,\alpha} - \lambda' v_{\alpha,\alpha}v_{\beta,\beta} - 2\mu' d_{\alpha\beta}d_{\alpha\beta} - k'T_{,\alpha\alpha} = 0 \qquad (3.3\text{-}13)$$

The Functional

In the following, the form of the functional in Eq. 3.2-7 corresponding to the preceding equations is given. The boundary conditions are extracted from the volume integral by integration by parts of the stresses and the temperature. In addition, adjoint boundary functions are added to enhance the appearance of symmetry. Let V_F denote the fluid volume and S its surface. S_{F_2} is that part of S where tractions $\hat{t}_\alpha$ are specified and S_{F_2} that part where the heat flux $\hat{q}_\alpha$ is specified.

The functional is given by

$$I = \int_{t_1}^{t_2} \int_{V_F} \{v_\alpha^* \rho \frac{Dv_\alpha}{Dt} + \lambda v_{\alpha,\alpha}^* v_{\beta,\beta} + 2\mu d_{\alpha\beta}^* d_{\alpha\beta} - RT\rho v_{\alpha,\alpha}^* -$$

$$- v_\alpha^* \rho f_\alpha + \rho^* \frac{D\rho}{Dt} + \rho^* \rho v_{\alpha,\alpha} + T^* C_v \frac{DT}{Dt} + T^* RT v_{\alpha,\alpha} -$$

$$- T^* \lambda' v_{\alpha,\alpha} v_{\beta,\beta} - T^* 2u' d_{\alpha\beta} d_{\alpha\beta} + k' T_{,\alpha}^* T_{,\alpha}\} \, dVdt -$$

$$- \int_{t_1}^{t_2} \int_{S_{F_2}} \{v_\alpha^* \hat{t}_\alpha + v_\alpha \hat{t}_\alpha^*\} \, dSdt +$$

$$+ \int_{t_1}^{t_2} \int_{S_{F_2}} \{T^* \hat{q}_\alpha n_\alpha + T \hat{q}_\alpha^* n_\alpha\} \, dSdt \qquad (3.3\text{-}14)$$

The Euler Equations and Boundary Conditions

For the functional defined in Eq. 3.3-14, the Euler equations in the primary variables are

$$\delta v_\alpha^*: \quad \rho \frac{Dv_\alpha}{Dt} - \lambda v_{\beta,\beta\alpha} - 2\mu d_{\alpha\beta,\beta} + (RT\rho)_{,\alpha} - \rho f_\alpha = 0 \qquad (3.3\text{-}15a)$$

$$\delta \rho^*: \quad \frac{D\rho}{Dt} + \rho v_{\alpha,\alpha} = 0 \qquad (3.3\text{-}15b)$$

$$\delta T^*: \quad C_v \frac{DT}{Dt} + RT v_{\alpha,\alpha} - \lambda' v_{\alpha,\alpha} v_{\beta,\beta} - 2\mu' d_{\alpha\beta} d_{\alpha\beta} - k' T_{,\alpha\alpha} = 0 \qquad (3.3\text{-}15c)$$

The remaining Euler equations, mixed in the primary variables and the adjoint variables, are

$$\delta v_\alpha: \quad (v_\alpha^* \rho)_{,t} + (v_\alpha^* \rho v_\beta)_{,\beta} + \lambda v^*_{\beta,\beta\alpha} + 2\mu d^*_{\alpha\beta,\beta} + p^*_{,\alpha}\rho +$$

$$+ (RT^*T)_{,\alpha} - 2\lambda'(T^* v_{\beta,\beta})_{,\alpha} - 4\mu'(T^* d_{\alpha\beta})_{,\beta} -$$

$$- v^*_\beta \rho v_{\beta,\alpha} - T^* C_v T_{,\alpha} = 0 \qquad (3.3\text{-}15d)$$

$$\delta\rho: \quad \rho^*_{,t} - v^*_\alpha \frac{Dv_\alpha}{Dt} + v^*_\alpha f_\alpha + RT v^*_{\alpha,\alpha} + v_\alpha p^*_{,\alpha} = 0 \qquad (3.3\text{-}15e)$$

$$\delta T: \quad C_v T^*_{,t} + (T^* C_v v_\beta)_{,\beta} + R\rho v^*_{\alpha,\alpha} - RT^* v_{\alpha,\alpha} +$$

$$+ k T^*_{,\alpha\alpha} = 0 \qquad (3.3\text{-}15f)$$

The boundary conditions are

$$\text{on } S_{F_2}: \quad \lambda v_{\beta,\beta} n_\alpha + 2\mu d_{\alpha\beta} n_\beta - RT\rho n_\alpha = \hat{t}_\alpha \qquad (3.3\text{-}16a)$$

$$\lambda v^*_{\beta,\beta} n_\alpha + 2\mu d^*_{\alpha\beta} n_\beta + v^*_\alpha \rho v_\beta n_\beta + p^* \rho n_\alpha +$$

$$+ T^*(RT n_\alpha - 2\lambda' v_{\beta,\beta} n_\alpha - 4\mu' d_{\alpha\beta} n_\beta) = \hat{t}^*_\alpha \qquad (3.3\text{-}16b)$$

$$\text{on } S_{F_2}: \quad -k' T_{,\alpha} n_\alpha = \hat{q}_\alpha n_\alpha \qquad (3.3\text{-}16c)$$

$$-k' T^*_{,\alpha} n_\alpha - T^* C_v v_\alpha n_\alpha = \hat{q}^*_\alpha n_\alpha \qquad (3.3\text{-}16d)$$

3.4 Inviscid Isentropic Fluid

Assumptions and Constitutive Equations

This fluid model is a special case of the compressible Newtonian fluid discussed in the preceding section. Since this model is used frequently in various analyses, its assumptions, equations and functional will be written here explicitly.

The assumption of negligible viscosity is expressed by setting the constants λ and μ of the Newtonian fluid model equal to zero. Consequently, the viscous stress tensor $t_{\alpha\beta}$ vanishes identically.

The equation of state for a perfect gas is

$$p = \rho RT \tag{3.4-1}$$

With the assumption of perfect behavior the entropy function is given by

$$S(p,\rho) = \frac{R}{\gamma-1} \log \frac{p}{\rho^{\gamma}} \tag{3.4-2}$$

Again, C_p is the specific heat at constant pressure, C_v is the specific heat at constant volume and

$$R = C_p - C_v \tag{3.4-3}$$

$$\gamma = C_p/C_v \tag{3.4-4}$$

The isentropic assumption for a moving fluid takes the form

$$\frac{DS}{Dt} = 0 \tag{3.4-5}$$

Thus the energy equation in terms of entropy

$$T \frac{DS}{Dt} = - \frac{1}{\rho} q_{\alpha,\alpha} \qquad (3.4\text{-}6)$$

leads to $q_{\alpha,\alpha} = 0$ or no heat conduction.

Body forces will not be considered, but may easily be included.

Full slip will be assumed at all boundaries, and only the normal velocity of the fluid will be prescribed.

It will be assumed that the internal energy per unit mass, E, is a function of temperature only, in the form

$$E = C_v T \qquad (3.4\text{-}7)$$

Governing Differential Equations

Without viscous stresses, the equations of motion reduce to

$$\rho \frac{Dv_\alpha}{Dt} + (RT\rho)_{,\alpha} = 0 \qquad (3.4\text{-}8)$$

when the perfect gas law is used to eliminate the pressure.

The continuity equation is

$$\frac{D\rho}{Dt} + \rho v_{\alpha,\alpha} = 0 \qquad (3.4\text{-}9)$$

With the isentropic assumption and the lack of dissipation, the temperature equation is simply

$$C_v \frac{DT}{Dt} + RTv_{\alpha,\alpha} = 0 \qquad (3.4\text{-}10)$$

The Functional

Insertion of the preceding equations into Eq. 3.2-7 leads to the functional to be presented in the following. Without the viscous stresses and heat conduction, integration by parts is performed only on the pressure gradient. Thus, the only surface integral in the functional contains a specified pressure.

The inviscid isentropic flow functional is

$$I = \int_{t_1}^{t_2} \int_{V_F} \left[v_\alpha^* \rho \frac{Dv_\alpha}{Dt} - RT\rho v_{\alpha,\alpha}^* + \rho^* \frac{D\rho}{Dt} + \rho^* \rho v_{\alpha,\alpha} + \right.$$

$$\left. + T^* C_v \frac{DT}{Dt} + T^* R T v_{\alpha,\alpha} \right] dV\,dt -$$

$$- \int_{t_1}^{t_2} \int_{S_{F_2}} \left[v_\alpha^* \hat{p} n_\alpha + v_\alpha \hat{p}^* n_\alpha \right] dS\,dt \qquad (3.4\text{-}11)$$

The Euler Equations and Boundary Conditions

For the functional defined by Eq. 3.4-11, the Euler equations on the primary variables are:

$$\delta v_\alpha^*: \quad \rho \frac{Dv_\alpha}{Dt} + (RT\rho)_{,\alpha} = 0 \qquad (3.4\text{-}12a)$$

$$\delta \rho^*: \quad \frac{D\rho}{Dt} + \rho v_{\alpha,\alpha} = 0 \qquad (3.4\text{-}12b)$$

$$\delta T^*: \quad C_v \frac{DT}{Dt} + RT v_{\alpha,\alpha} = 0 \qquad (3.4\text{-}12c)$$

The Euler equations, mixed in the primary and adjoint variables, are

$$\delta V_\alpha: \quad -\frac{D(V_\alpha^* \rho)}{Dt} - \rho V_\alpha^* V_{\beta,\beta} + \rho V_\beta^* V_{\beta,\alpha} -$$

$$-\rho \rho^*_{,\alpha} + T^* C_v T_{,\alpha} - (T^* R T)_{,\alpha} = 0 \qquad (3.4\text{-}12d)$$

$$\delta \rho: \quad -\frac{D\rho^*}{Dt} + V_\alpha^* \frac{DV_\alpha}{Dt} - RT V^*_{\alpha,\alpha} = 0 \qquad (3.4\text{-}12e)$$

$$\delta T: \quad -C_v \frac{DT^*}{Dt} - C_v T^* V_{\alpha,\alpha} + R T^* V_{\alpha,\alpha} - R\rho V^*_{\alpha,\alpha} = 0 \qquad (3.4\text{-}12f)$$

The boundary conditions are

$$\text{on } S_{F_2}: \quad RT\rho n_\alpha = \hat{p} n_\alpha \qquad (3.4\text{-}13a)$$

$$V_\alpha^* \rho V_\beta n_\beta + T^* R T n_\alpha + \rho^* \rho n_\alpha = \hat{p}^* n_\alpha \qquad (3.4\text{-}13b)$$

3.5 Elastic Solid

The equations for thermodynamics of an elastic solid are presented here only for completeness. The functional given in this section is not that of the Principle of Minimum Total Potential Energy but instead is the adjoint functional constructed by the present method. An example will be given in a subsequent chapter of an elastic membrane with geometric non-linearities. It will be shown that, in this case, the results are identical to those of the Principle.

The Constitutive Equations

Let U be the internal energy per unit mass, T the temperature, and S, the entropy per unit mass. The free energy A is defined as

$$A = U - ST \tag{3.5-1}$$

For a linear elastic material, the free energy will be

$$\rho_0 A = \frac{1}{2}\lambda (e_{aa})^2 + \mu e_{ab}e_{ab} - \beta T e_{aa} - \frac{1}{2}\gamma T^2 \tag{3.5-2}$$

where λ and μ are the Lamé constants, β is the pressure coefficient and γ is a specific heat parameter. Thus, the material stress tensor is found to be

$$s_{ab} = \rho_0 \frac{\partial A}{\partial e_{ab}} = \lambda e_{cc}\delta_{ab} + 2\mu e_{ab} - \beta T\delta_{ab} \tag{3.5-3}$$

Further, the entropy function is given by

$$S = -\frac{\partial A}{\partial T} = \frac{1}{\rho_0}\beta e_{aa} + \frac{1}{\rho_0}\gamma T \tag{3.5-4}$$

In the above, the material strain tensor is

$$e_{ab} = \frac{1}{2} (u_{a,b} + u_{b,a} + u_{c,a}u_{c,b}) \qquad (3.5\text{-}5)$$

The heat conduction law is assumed in the form

$$q_{0_a} = - kT,_a \qquad (3.5\text{-}6)$$

where q_{0_a} is the heat flux vector, and k is the thermal conductivity.

Governing Differential Equations

The Equation of Motion

The equation of motion for the elastic solid in material coordinates is assumed in the form

$$[s_{ab}(\delta_{cb} + u_{c,b})],_a + \rho_0 f_c - \rho_0 a_c = 0 \qquad (3.5\text{-}7)$$

where f_c is the body force vector per unit mass, and a_c is the acceleration vector.

The Temperature Equation

The local form of the First Law of Thermodynamics minus the rate of change of mechanical energy, in material coordinates, is

$$\rho_0 \dot{U} - s_{ab}\dot{e}_{ab} + q_{0_{a,a}} - \rho_0 r = 0 \qquad (3.5\text{-}8)$$

The rate of change of internal energy $\dot{U}$, can be expressed in terms of the free energy A, entropy S and temperature T, as follows:

$$\dot{U} = \dot{A} + \dot{S}T + S\dot{T} = \frac{\partial A}{\partial T}\dot{T} + \frac{\partial A}{\partial e_{ab}}\dot{e}_{ab} + \dot{S}T + S\dot{T}$$

$$= \dot{S}T + \frac{1}{\rho_0} s_{ab}\dot{e}_{ab} \qquad (3.5\text{-}9)$$

With this substitution for $\dot{U}$, the energy equation becomes

$$\rho_0 \dot{S}T + q_{0_{a,a}} - \rho_0 r = 0 \qquad (3.5\text{-}10)$$

For the specific free energy function given, the entropy rate is

$$\dot{S} = \frac{1}{\rho_0}\beta\dot{e}_{aa} + \frac{1}{\rho_0}\gamma\dot{T} \qquad (3.5\text{-}11)$$

and the equation takes the form

$$\gamma T\dot{T} - kT_{,aa} - \rho_0 r + \beta T\dot{e}_{aa} = 0 \qquad (3.5\text{-}12)$$

The Functional

The functional presented here is obtained from Eq. 3.2-7 by insertion of the preceding equations. It differs from the Principle of Minimum Total Potential Energy primarily in the inclusion of the temperature equation. Integration by parts is performed on the acceleration, the strain rate term in the temperature equation, the stresses and the heat flux gradient. The latter two will contribute to the boundary conditions on S_{S_2} and S_{S_2}, respectively, after the variation. The specified adjoint boundary functions are included to enhance the appearance of symmetry.

The functional I is defined by

$$I = \int_{t_1}^{t_2}\int_{V_S} [-u^*_{c,a} S_{ab}(\delta_{cb} + u_{c,b}) + u^*_c \rho_o f_c + \rho_o \dot{u}^*_c \dot{u}_c +$$

$$+ kT^*_{,a} T_{,a} + \gamma T^* T\dot{T} - \rho_o T^* r - \beta e_{aa}(T^* T)_{,t}]\, dV\, dt +$$

$$+ \int_{t_1}^{t_2}\int_{S_{S_2}} [\, u^*_c \hat{t}_c + u_c \hat{t}^*_c\,]\, dS\, dt +$$

$$+ \int_{t_1}^{t_2}\int_{S_{S_2}} [\, T^* \hat{q}_a n_a + T \hat{q}^*_a n_a]\, dS\, dt \qquad (3.5\text{-}13)$$

Euler Equations and Boundary Conditions

For the functional defined in Eq. 3.5-13, the Euler equations in the primary variables are

$$\delta u^*_c : [S_{ab}(\delta_{cb} + u_{c,b})]_{,a} + \rho_o f_c - \rho_o \ddot{u}_c = 0 \qquad (3.5\text{-}14a)$$

$$\delta T^* : \gamma T\dot{T} - kT_{,aa} - \rho_o r + \beta \dot{e}_{aa} T = 0 \qquad (3.5\text{-}14b)$$

The Euler equations, mixed in primary and adjoint variables, are

$$\delta u_c : [u^*_{c,a} S_{ab} + (\delta_{cf} + u_{cf})\{\lambda \delta_{bf}(u^*_{a,a} + u^*_{a,d} u_{a,d}) +$$

$$+ \mu(u^*_{b,f} + u^*_{f,b} + u^*_{a,f} u_{a,b} + u_{a,f} u^*_{a,b}) -$$

$$- \beta(TT^*)_{,t} \delta_{bf}\}]_{,b} - \ddot{u}^*_c = 0 \qquad (3.5\text{-}14c)$$

$$\delta T : -\gamma T\dot{T}^* - kT^*_{,aa} + \beta \dot{e}_{aa} T^* = 0 \qquad (3.5\text{-}14d)$$

The boundary equations are

$$\text{on } S_{S_2}: \quad S_{ab}(\delta_{ab} + u_{c,b})\, n_a = \hat{t}_c \tag{3.5-15a}$$

$$u^*_{c,a} S_{ab} n_b + (\delta_{cf} + u_{c,f})\left[\lambda \delta_{bf}(u^*_{a,a} + u^*_{a,d} u_{a,d}) + \right.$$

$$+ \mu(u^*_{b,f} + u^*_{f,b} + u^*_{a,f} u_{a,b} + u_{a,f} u^*_{a,b}) -$$

$$\left. - \beta(TT^*)_{,t} \delta_{bf}\right] n_b = \hat{t}^*_c \tag{3.5-15b}$$

$$\text{on } S_{S_2}: \quad -k T_{,a} n_a = \hat{q}_a n_a \tag{3.5-15c}$$

$$-k T^*_{,a} n_a = \hat{q}^*_a n_a \tag{3.5-15d}$$

3.6 Variational Principle for Fluid Structure Interaction

The functional for fluid structure interaction to be presented in this section is constructed from the governing differential equations of each region. The condition of continuity on the interface is expressed as an admissibility requirement on the trial functions and, therefore, does not appear in the functional.

In the following, general coordinates have been used with the vertical bar signifying covariant differentiation, and the metric tensor denoted by g_{ab} or $g_{\alpha\beta}$. The use of general coordinates in this principle is a simple extension of the previous sections and is justified solely on the grounds that it contributes greatly to the generality of the formulation.

Consider the region R divided into two volumes, V_F and V_S and bounded by surface S (Fig. 3.1). Let V_S be that part of the region containing the structure. The portion of S bounding V_S is S_S. The remaining part of the region, V_F, contains the fluid. The portion of S bounding V_F is S_F. The surface S will be partitioned two ways: first, $S_{S_1}, S_{S_2}, S_{F_1}, S_{F_2}$; and second, $S_{S_1}, S_{S_2}, S_{F_1}, S_{F_2}$. Each partition will account for the entire surface S.

Make stationary, the functional

$$
\begin{aligned}
I = \int_{t_1}^{t_2} \int_{V_S} \Big[& -u^*_{c|a}\, s^{ab} (g^c{}_b + u^c{}_{|b}) + u^*_c \rho_o f^c + \rho_o \dot{u}^*_c \dot{u}^c + \\
& + k T^*_{,a} T_{,b} g^{ab} + T^* \gamma T \dot{T} - \rho_o r T^* - \\
& - T^* \beta e^a{}_a (T T^*)_{,t} \Big] dV\, dt + \\
& + \int_{t_1}^{t_2} \int_{V_F} \Big[v^*_\alpha \rho \frac{D v_\alpha}{D t} - v^*_\alpha \rho f^\alpha + \lambda v^{*\alpha}{}_{|\alpha} v^\beta{}_{|\beta} + \\
& + 2\mu d^*_{\alpha\beta} d^{\alpha\beta} - R T \rho v^{*\alpha}{}_{|\alpha} + \rho^* \frac{D \rho}{D t} + \rho^* \rho v^\alpha{}_{|\alpha} + \\
& + T^* C_v \frac{D T}{D t} + R T^* T v^\alpha{}_{|\alpha} - \lambda' T^* v^\alpha{}_{|\alpha} v^\beta{}_{|\beta} - \\
& - 2\mu' T^* d_{\alpha\beta} d^{\alpha\beta} + k' T^*_{|\alpha} T_{|\beta} g^{\alpha\beta} \Big] dV dt + \\
& + \int_{t_1}^{t_2} \int_{S_{S_2}} \Big[u^*_c \hat{t}^c + u^c \hat{t}^*_c \Big] dS\, dt + \\
\end{aligned}
$$

$$+ \int_{t_1}^{t_2} \int_{S_{F_2}} [T^* \hat{q}^{\alpha} n_{\alpha} + T \hat{q}^{*\alpha} n_{\alpha}] dS dt -$$

$$- \int_{t_1}^{t_2} \int_{S_{F_2}} [v_{\alpha}^* \hat{t}^{\alpha} + v^{\alpha} \hat{t}_{\alpha}^*] dS dt +$$

$$+ \int_{t_1}^{t_2} \int_{S_{F_2}} [T^* \hat{q}_{\alpha} n^{\alpha} + T \hat{q}^{*\alpha} n_{\alpha}] dS dt \qquad (3.6\text{-}1)$$

among functions u^c, u_c^*, T, T^*, continuous and defined on V_S and S_S, satisfying

$$u^c = \hat{u}^c, \quad u_c^* = \hat{u}_c^* \quad \text{on } S_{S_1} \qquad (3.6\text{-}2a)$$

$$T = \hat{T}, \quad T^* = \hat{T}^* \quad \text{on } S_{S_1} \qquad (3.6\text{-}2b)$$

and among functions $v^{\alpha}, v_{\alpha}^*, \rho, \rho^*, T, T^*$, continuous and defined on V_F and S_F, satisfying

$$v^{\alpha} = \hat{v}^{\alpha}, \quad v^{*\alpha} = \hat{v}^{*\alpha} \quad \text{on } S_{F_1} \qquad (3.6\text{-}3a)$$

$$T = \hat{T}, \quad T^* = \hat{T}^* \quad \text{on } S_{F_1} \qquad (3.6\text{-}3b)$$

where

$$\frac{D\cdot}{Dt} = \frac{\partial \cdot}{\partial t} + v^{\beta} \cdot_{|\beta} \qquad (3.6\text{-}4)$$

Further, let the interface S_I be the common boundary between V_S and V_F. Admissible structural velocities and fluid velocities must be continuous across S_I, and admissible fluid temperatures and structural temperatures must be continuous across S_I.

Stationarity of this functional is equivalent to the satisfaction of the governing differential equations and assures continuity of the traction vector across S_I.

4. NUMERICAL METHOD FOR INVISCID COMPRESSIBLE FLUID AND AN ELASTIC SOLID

4.1 Spatial Discretization of the Fluid Functional

Matrix Equations

Proceeding by the finite element method, the fluid volume, V_F, is subdivided into elements of volume V_{F_e}, such that there is no gapping or overlapping, and the entire volume is included. The functional I will be taken as the sum over all elements of the element functionals I_e.

Within each element, the variables will be approximated by the product of interpolation functions and nodal parameters. These parameters will be taken to be the value of the variable at the spatial point or node of the element.

Specifically, the approximations are

$$\begin{aligned} v_\alpha^* &= N_i^* v_{\alpha_i}^* & v_\alpha &= N_i v_{\alpha_i} \\ \rho^* &= L_i^* \rho_i^* & \rho &= L_i \rho_i \\ T^* &= M_i^* T_i^* & T &= M_i T_i \end{aligned} \qquad (4.1\text{-}1)$$

Notice that the following two expressions are equivalent:

$$v_\alpha^* = N_i^* v_{\alpha_i}^* \qquad v_\alpha^* = [N^*]\ \{v^*\}$$

The vector of nodal velocity parameters $\{v\}$ will be ordered in coordinate sequence by node. Let $[N_{xy}]$ be a row matrix such that

$$v_{\alpha,\alpha} = [N_{xy}] \{v\} \tag{4.1-2}$$

Then the elemental functional becomes

$$\begin{aligned}
I_e = &\int_{t_1}^{t_2}\int_{V_{F_e}} \{v^*\}^T [N^*]^T [N] \{\dot{v}\} [L] \{\rho\} \, dV dt + \\
&+ \int_{t_1}^{t_2}\int_{V_{F_e}} \{v^*\}^T [N^*]^T \left[[N_{,x}] \{v\} \vdots [N_{,y}] \{v\} \right] [N] \{v\} [L] \{\rho\} \, dV dt - \\
&- \int_{t_1}^{t_2}\int_{V_{F_e}} \{v^*\}^T [N_{xy}^*]^T [M] \{T\} R [L] \{\rho\} \, dV dt + \\
&+ \int_{t_1}^{t_2}\int_{V_{F_e}} \{\rho^*\}^T [L^*]^T [L] \{\dot{\rho}\} \, dV dt + \\
&+ \int_{t_1}^{t_2}\int_{V_{F_e}} \{\rho^*\}^T [L^*]^T \left[[L_{,x}] \{\rho\} \vdots [L_{,y}] \{\rho\} \right] [N] \{v\} \, dV dt + \\
&+ \int_{t_1}^{t_2}\int_{V_{F_e}} \{\rho^*\}^T [L^*]^T [L] \{\rho\} [N_{xy}] \{v\} \, dV dt + \\
&+ \int_{t_1}^{t_2}\int_{V_{F_e}} \{T^*\}^T [M^*]^T [M] \{\dot{T}\} \, dV dt + \\
&+ \int_{t_1}^{t_2}\int_{V_{F_e}} \{T^*\}^T [M^*]^T \left[[M_{,x}] \{T\} \vdots [M_{,y}] \{T\} \right] [N] \{v\} \, dV dt + \\
&+ \int_{t_1}^{t_2}\int_{V_{F_e}} \{T^*\}^T [M^*]^T \frac{R}{C_v} [M] \{T\} [N_{xy}] \{v\} \, dV dt - \\
&- \int_{t_1}^{t_2}\int_{S_{F_e}} \{v^*\}^T [N^*]^T \{n\} \hat{p} \, dS dt
\end{aligned} \tag{4.1-3}$$

Due to the linearity of the functional in the adjoint variables, enforcing stationarity with respect to the adjoint nodal parameters leads to equations in the primary nodal variables only. The stationarity is expressed by

$$\frac{\partial I}{\partial \{v^*\}} = 0; \qquad \frac{\partial I}{\partial \{\rho^*\}} = 0; \qquad \frac{\partial I}{\partial \{T^*\}} = 0 \tag{4.1-4}$$

and the resulting equations are

$$[VM]\{\dot{v}\} + [VV]\{v\} - \{P\} = 0 \tag{4.1-5a}$$

$$[RM]\{\dot{\rho}\} + [RV]\{v\} = 0 \tag{4.1-5b}$$

$$[TM]\{\dot{T}\} + [TV]\{v\} = 0 \tag{4.1-5c}$$

These global matrices have been assembled by standard techniques from the following element matrices:

$$[VM]_e = \int_{V_{F_e}} [L]\{\rho\}[N^*]^T[N]\,dV \tag{4.1-6a}$$

$$[VV]_e = \int_{V_{F_e}} [L]\{\rho\}\left[[N_{,x}]\{v\}_i : [N_{,y}]\{v\}_i\right][N]\,dV \tag{4.1-6b}$$

$$\{P\}_e = \int_{V_{F_e}} [N^*_{xy}]^T[M]\{T\}R[L]\{\rho\}\,dV + \int_{S_{F_e}} [N^*]^T\{n\}\hat{p}\,dS \tag{4.1-6c}$$

$$[RM]_e = \int_{V_{F_e}} [L^*]^T[L]\,dV \tag{4.1-6d}$$

$$[TM]_e = \int_{V_{F_e}} [M^*]^T[M]\,dV \tag{4.1-6e}$$

$$[RV]_e = \int_{V_{Fe}} \left\{ [L^*]^T \left[[L_{,x}]\{p\} \; ; \; [L_{,y}]\{p\} \right] [N] + [L^*]^T [L] \{p\} [N_{,v}] \right\} dV \qquad (4.1\text{-}6f)$$

$$[TV]_e = \int_{V_{Fe}} \left\{ [M^*]^T \left[[M_{,x}]\{T\} \; ; \; [M_{,y}]\{T\} \right] [N] + [M^*]^T \frac{R}{C_v} [M] \{T\} [N_{,v}] \right\} dV \qquad (4.1\text{-}6g)$$

The Bilinear Quadrilateral Fluid Element

The isoparametric quadrilateral with linear interpolation functions was chosen since it is the lowest order quadrilateral that will produce a continuous variable field. The element matrices are evaluated by numerical integration using a two point Gaussian quadrature in each coordinate. The mapping functions and all variable interpolaton functions were chosen to be

$$N_i = \frac{1}{4} (1 + \xi\xi_i) \; (1 + \eta\eta_i) \qquad i = 1,2,3,4 \qquad (4.1.7)$$

The end product of the element routine is an elemental contribution to the global rate vector. Given the current value of the nodal parameters, the element contributions are calculated and summed by connectivity. Lumped masses are used to simplify the procedure.

4.2 Upwind Weighting

Convected Inertia Terms

The recent work of Heinrich, Huyakorn, Mitchell and Zienkiewicz (1977) forms the basis for the present

use of upwind weighting in finite elements. The authors have established the nature of the numerical instability associated with one-dimensional transport problems. By employing an asymmetric or "upwind weighted element," they were able to demonstrate the values of the winding parameter that lead to unstable solutions to the difference equations. Their work indicates that large coefficients of the gradients are the source of the instability.

The equation solution is stabilized by modifying the weighting functions of a weighted residual method. For example, for a one-dimensional element, the weighting functions are

$$W_i = W_i(x,\alpha) = N_i(x) + \alpha F(x) \qquad (4.2\text{-}1)$$

The authors chose

$$F(x) = -\frac{3}{h^2}\, x(x-h) \qquad (4.2\text{-}2)$$

where h is the mesh size (Fig. 4.1). The effect of the upwinding is to shift the elemental emphasis to the direction of upwind. This is accomplished by giving α the sign of the velocity v along the element. Their work shows that a certain value of α will lead to minimum error in the difference equations. A sizable reduction in error is reported when using an optimal value of upwinding instead of full upwinding.

The authors have carried their numerical work to

two dimensions although it was not possible to extend the analytical work. Since two-dimensional interpolation functions are formed from products of one-dimensional interpolation functions, the two-dimensional weighting functions are formed similarly. Introducing β as an η direction winding parameter, the functions for the bilinear isoparametric quadrilateral are

$$N_i = \frac{1}{2}(1+\xi\xi_i)\frac{1}{2}(1+\eta\eta_i) \tag{4.2-3}$$

$$W_i = \left[\frac{1}{2}(1+\xi\xi_i)+\frac{3}{4}\alpha(1+\xi)(1-\xi)\right]\left[\frac{1}{2}(1+\eta\eta_i)+\frac{3}{4}\beta(1+\eta)(1-\eta)\right] \tag{4.2-4}$$

Notice that these weighting functions reduce to the interpolation functions for the case of no winding. The authors note that, in a true method of weighted residuals fashion, these winded weighting functions are applied to all terms in the residual. The analogous development for the present set of nonlinear equations has not been demonstrated.

Typical Nodal Equation in One Dimension

To see the effects of upwind weighting when used in the present set of nonlinear equations, the typical nodal equation for a one-dimensional assemblage of elements will be presented. The elements are line elements of unit length using linear interpolation functions. The upwind weighting functions will be applied to the convected gradient terms only.

Consider two line elements of unit length. Let the common node be labeled 2, the upwind node be 1, and the downwind node be 3. Each node will have three nodal parameters: u_i, ρ_i, T_i. By straightforward evaluation of the matrix equations, the three typical nodal equations are found to be

$$\left(\tfrac{1}{12}\rho_1+\tfrac{1}{12}\rho_2\right)\dot{V}_1 + \left(\tfrac{1}{12}\rho_1+\tfrac{1}{2}\rho_2+\tfrac{1}{12}\rho_3\right)\dot{V}_2 + \left(\tfrac{1}{12}\rho_2+\tfrac{1}{12}\rho_3\right)\dot{V}_3 +$$

$$+(V_2-V_1)\left[\tfrac{1}{12}\rho_1\left(1+\tfrac{9}{5}\alpha\right)+\tfrac{1}{12}\rho_2\left(1+\tfrac{6}{5}\alpha\right)\right]V_1 +$$

$$+\left\{(V_2-V_1)\left[\tfrac{1}{12}\rho_1\left(1+\tfrac{6}{5}\alpha\right)+\tfrac{1}{4}\rho_2\left(1+\tfrac{3}{5}\alpha\right)\right]+(V_3-V_2)\left[\tfrac{1}{4}\rho_2\left(1-\tfrac{3}{5}\alpha\right)+\right.\right.$$

$$\left.\left.+\tfrac{1}{12}\rho_3\left(1-\tfrac{6}{5}\alpha\right)\right]\right\}V_2 + (V_3-V_2)\left[\tfrac{1}{12}\rho_2\left(1-\tfrac{6}{5}\alpha\right)+\tfrac{1}{12}\rho_3\left(1-\tfrac{9}{5}\alpha\right)V_3 -\right.$$

$$-R\left(\tfrac{1}{3}T_1\rho_1+\tfrac{1}{6}T_2\rho_2+\tfrac{1}{6}T_1\rho_2-\tfrac{1}{6}T_2\rho_3-\tfrac{1}{6}T_3\rho_2-\tfrac{1}{3}T_3\rho_3\right)=0$$

(4.2-5a)

$$\tfrac{1}{6}\dot{\rho}_1+\tfrac{2}{3}\dot{\rho}_2+\tfrac{1}{6}\dot{\rho}_3+\tfrac{1}{6}(\rho_2-\rho_1)\left(1+\tfrac{3}{2}\alpha\right)V_1+\left\{\tfrac{1}{3}(\rho_2-\rho_1)\left(1+\tfrac{3}{4}\alpha\right)+\right.$$

$$\left.+\tfrac{1}{3}(\rho_3-\rho_2)\left(1-\tfrac{3}{4}\alpha\right)\right\}V_2+\tfrac{1}{6}(\rho_3-\rho_2)\left(1-\tfrac{3}{2}\alpha\right)V_3 -$$

$$-\left(\tfrac{1}{6}\rho_1+\tfrac{1}{3}\rho_2\right)V_1+\left(\tfrac{1}{6}\rho_1-\tfrac{1}{6}\rho_3\right)V_2+\left(\tfrac{1}{3}\rho_2+\tfrac{1}{6}\rho_3\right)V_3=0$$

(4.2-5b)

$$\frac{1}{6}\dot{T}_1 + \frac{2}{3}\dot{T}_2 + \frac{1}{6}\dot{T}_3 + \frac{1}{6}(T_2 - T_1)(1 + \frac{3}{2}\alpha)V_1 + \left\{\frac{1}{3}(T_2 - T_1)(1 + \frac{3}{4}\alpha) + \right.$$

$$\left. + \frac{1}{3}(T_3 - T_2)(1 - \frac{3}{4}\alpha)\right\}V_2 + \frac{1}{6}(T_3 - T_2)(1 - \frac{3}{2}\alpha)V_3 -$$

$$- \frac{R}{C_v}\left(\frac{1}{6}T_1 + \frac{1}{3}T_2\right)V_1 + \frac{R}{C_v}\left(\frac{1}{6}T_1 - \frac{1}{6}T_3\right)V_2 + \frac{R}{C_v}\left(\frac{1}{3}T_2 + \frac{1}{6}T_3\right)V_3 = 0$$

(4.2-5c)

For a local velocity positive, or from node 1 to node 3, $\alpha = 1.0$. The gradients from the left or upwind element receive a greater weight than corresponding gradients from the downwind element. In the momentum equation, the upwind gradient, $v_2 - v_1$, has weight increased by α, that part including ρ_1 receiving the largest. The downwind gradient, $v_3 - v_2$, receives diminished weight when multiplied by v_2, and even further reduced weight when multiplied by v_3. In both terms, ρ_2 receives more weight than ρ_3. For negative velocities, $\alpha = -1.0$ and all effects are reversed.

Typical Nodal Equation in Two Dimensions

When implementing upwind weighting in two dimensions, several additional effects occur. Because of the multiplicative generation of the weighting functions, the y direction winding affects the x direction equations substantially. Thus, when considering a flow with a

dominant velocity direction, the concept of cross winding arises. Velocity in this cross direction significantly affects the response of the main flow.

To see this, partial sums of terms from a typical nodal equation will be presented. The elements used will be bilinear squares with unit length sides (Fig. 4.2a). All nodal parameters will be interpolated linearly and all variables will use the same interpolation functions. Upwind weighting will only be applied to the convected terms.

The interpolation functions are

$$N_1 = (1-x)(1-y)$$

$$N_2 = (x)\ (1-y)$$

$$N_3 = (x)\ (y)$$

$$N_4 = (1-x)\ (y) \qquad (4.2\text{-}6)$$

The weighting functions are

$$W_1 = [(1-x) - 3\alpha x(1-x)][(1-y) - 3\beta y(1-y)]$$

$$W_2 = [\ x\ + 3\alpha x(1-x)][(1-y) - 3\beta y(1-y)]$$

$$W_3 = [\ x\ + 3\alpha x(1-x)][\ y\ + 3\beta y(1-y)]$$

$$W_4 = [(1-x) - 3\alpha x(1-x)][\ y\ + 3\beta y(1-y)] \qquad (4.2\text{-}7)$$

To see the interaction of winding in the two directions, consider the nodal equations for two elements with a common side (Fig. 4.2b). The equation for v_x at node 3 contains convected inertia terms that are quadratic in the velocities from all nodes. For purposes of comparison, terms in $v_{x_3}^2, v_{x_3} v_{x_4}, v_{x_4}^2$ from the v_{x_3} and v_{x_4} equations will be listed.

From the v_{x_3} equation, the terms are

$$
\begin{aligned}
\ldots + V_{x_3} V_{x_3} \; & \Big\{ \left(\tfrac{1}{5} - \tfrac{1}{10}\beta\right)\left[\left(\tfrac{1}{12} + \tfrac{1}{10}\alpha\right)\rho_1 + \left(\tfrac{1}{4} + \tfrac{3}{20}\alpha\right)\rho_3\right] + \\
& + \left(\tfrac{1}{20} - \tfrac{1}{20}\beta\right)\left[\left(\tfrac{1}{4} + \tfrac{3}{20}\alpha\right)\rho_4 + \left(\tfrac{1}{12} + \tfrac{1}{10}\alpha\right)\rho_2\right] - \\
& - \left(\tfrac{1}{5} - \tfrac{1}{10}\beta\right)\left[\left(\tfrac{1}{4} - \tfrac{3}{20}\alpha\right)\rho_3 + \left(\tfrac{1}{12} - \tfrac{1}{10}\alpha\right)\rho_5\right] - \\
& - \left(\tfrac{1}{20} - \tfrac{1}{20}\beta\right)\left[\left(\tfrac{1}{12} - \tfrac{1}{10}\alpha\right)\rho_6 + \left(\tfrac{1}{4} - \tfrac{3}{20}\alpha\right)\rho_4\right] \Big\} + \\
+ V_{x_3} V_{x_4} \; & \Big\{ \left(\tfrac{1}{20} - \tfrac{1}{20}\beta\right)\left[\left(\tfrac{1}{12} + \tfrac{1}{10}\alpha\right)\rho_1 + \left(\tfrac{1}{4} + \tfrac{3}{20}\alpha\right)\rho_3\right] + \\
& + \left(\tfrac{1}{30} - \tfrac{1}{20}\beta\right)\left[\left(\tfrac{1}{4} + \tfrac{3}{20}\alpha\right)\rho_4 + \left(\tfrac{1}{12} + \tfrac{1}{10}\alpha\right)\rho_2\right] - \\
& - \left(\tfrac{1}{20} - \tfrac{1}{20}\beta\right)\left[\left(\tfrac{1}{4} - \tfrac{3}{20}\alpha\right)\rho_3 + \left(\tfrac{1}{12} - \tfrac{1}{10}\alpha\right)\rho_5\right] - \\
& - \left(\tfrac{1}{30} - \tfrac{1}{20}\beta\right)\left[\left(\tfrac{1}{12} - \tfrac{1}{10}\alpha\right)\rho_6 + \left(\tfrac{1}{4} - \tfrac{3}{20}\alpha\right)\rho_4\right] + \\
& + \left(\tfrac{1}{20} - \tfrac{1}{20}\beta\right)\left[\left(\tfrac{1}{12} + \tfrac{1}{10}\alpha\right)\rho_1 + \left(\tfrac{1}{4} + \tfrac{3}{20}\alpha\right)\rho_3\right] + \\
& + \left(\tfrac{1}{30} - \tfrac{1}{20}\beta\right)\left[\left(\tfrac{1}{4} + \tfrac{3}{20}\alpha\right)\rho_4 + \left(\tfrac{1}{12} + \tfrac{1}{10}\alpha\right)\rho_2\right] - \\
& - \left(\tfrac{1}{20} - \tfrac{1}{20}\beta\right)\left[\left(\tfrac{1}{4} - \tfrac{3}{20}\alpha\right)\rho_3 + \left(\tfrac{1}{12} - \tfrac{1}{10}\alpha\right)\rho_5\right] - \\
& - \left(\tfrac{1}{30} - \tfrac{1}{20}\beta\right)\left[\left(\tfrac{1}{12} - \tfrac{1}{10}\alpha\right)\rho_6 + \left(\tfrac{1}{4} - \tfrac{3}{20}\alpha\right)\rho_4\right] \Big\} + \\
+ V_{x_4} V_{x_4} \; & \Big\{ \left(\tfrac{1}{30} - \tfrac{1}{20}\beta\right)\left[\left(\tfrac{1}{12} + \tfrac{1}{10}\alpha\right)\rho_1 + \left(\tfrac{1}{4} + \tfrac{3}{20}\alpha\right)\rho_3\right] + \\
& + \left(\tfrac{1}{5} - \tfrac{1}{10}\beta\right)\left[\left(\tfrac{1}{4} + \tfrac{3}{20}\alpha\right)\rho_4 + \left(\tfrac{1}{12} + \tfrac{1}{10}\alpha\right)\rho_2\right] - \\
& - \left(\tfrac{1}{30} - \tfrac{1}{20}\beta\right)\left[\left(\tfrac{1}{4} - \tfrac{3}{20}\alpha\right)\rho_3 + \left(\tfrac{1}{12} - \tfrac{1}{10}\alpha\right)\rho_5\right] - \\
& - \left(\tfrac{1}{20} - \tfrac{1}{10}\beta\right)\left[\left(\tfrac{1}{12} - \tfrac{1}{10}\alpha\right)\rho_6 + \left(\tfrac{1}{4} - \tfrac{3}{20}\alpha\right)\rho_4\right] \Big\} + \ldots
\end{aligned}
\tag{4.2-8}
$$

From the v_{x_4} equation, the terms are

$$
\begin{aligned}
\ldots + V_{x_3} V_{x_3} \; & \Big\{ \left(\tfrac{1}{20}+\tfrac{1}{10}\beta\right)\left[\left(\tfrac{1}{12}+\tfrac{1}{10}\alpha\right)\rho_1 + \left(\tfrac{1}{4}+\tfrac{3}{20}\alpha\right)\rho_3\right] + \\
& + \left(\tfrac{1}{30}+\tfrac{1}{20}\beta\right)\left[\left(\tfrac{1}{4}+\tfrac{3}{20}\alpha\right)\rho_4 + \left(\tfrac{1}{12}+\tfrac{1}{10}\alpha\right)\rho_2\right] - \\
& - \left(\tfrac{1}{20}+\tfrac{1}{10}\beta\right)\left[\left(\tfrac{1}{4}-\tfrac{3}{20}\alpha\right)\rho_3 + \left(\tfrac{1}{12}-\tfrac{1}{10}\alpha\right)\rho_5\right] - \\
& - \left(\tfrac{1}{30}-\tfrac{1}{20}\beta\right)\left[\left(\tfrac{1}{12}-\tfrac{1}{10}\alpha\right)\rho_6 + \left(\tfrac{1}{4}-\tfrac{3}{20}\alpha\right)\rho_4\right] \Big\} + \\
+ V_{x_3} V_{x_4} \; & \Big\{ \left(\tfrac{1}{30}+\tfrac{1}{20}\beta\right)\left[\left(\tfrac{1}{12}+\tfrac{1}{10}\alpha\right)\rho_1 + \left(\tfrac{1}{4}+\tfrac{3}{20}\alpha\right)\rho_3\right] + \\
& + \left(\tfrac{1}{20}+\tfrac{1}{20}\beta\right)\left[\left(\tfrac{1}{4}+\tfrac{3}{20}\alpha\right)\rho_4 + \left(\tfrac{1}{12}+\tfrac{1}{10}\alpha\right)\rho_2\right] - \\
& - \left(\tfrac{1}{30}+\tfrac{1}{20}\beta\right)\left[\left(\tfrac{1}{4}-\tfrac{3}{20}\alpha\right)\rho_3 + \left(\tfrac{1}{12}-\tfrac{1}{10}\alpha\right)\rho_5\right] - \\
& - \left(\tfrac{1}{20}+\tfrac{1}{20}\beta\right)\left[\left(\tfrac{1}{12}-\tfrac{1}{10}\alpha\right)\rho_6 + \left(\tfrac{1}{4}-\tfrac{3}{20}\alpha\right)\rho_4\right] + \\
& + \left(\tfrac{1}{30}+\tfrac{1}{20}\beta\right)\left[\left(\tfrac{1}{12}+\tfrac{1}{10}\alpha\right)\rho_1 + \left(\tfrac{1}{4}+\tfrac{3}{20}\alpha\right)\rho_3\right] + \\
& + \left(\tfrac{1}{20}+\tfrac{1}{20}\beta\right)\left[\left(\tfrac{1}{4}+\tfrac{3}{20}\alpha\right)\rho_4 + \left(\tfrac{1}{12}+\tfrac{1}{10}\alpha\right)\rho_2\right] - \\
& - \left(\tfrac{1}{30}+\tfrac{1}{20}\beta\right)\left[\left(\tfrac{1}{4}-\tfrac{3}{20}\alpha\right)\rho_3 + \left(\tfrac{1}{12}-\tfrac{1}{10}\alpha\right)\rho_5\right] - \\
& - \left(\tfrac{1}{20}+\tfrac{1}{20}\beta\right)\left[\left(\tfrac{1}{12}-\tfrac{1}{10}\alpha\right)\rho_6 + \left(\tfrac{1}{4}-\tfrac{3}{20}\alpha\right)\rho_4\right] \Big\} + \\
+ V_{x_4} V_{x_4} \; & \Big\{ \left(\tfrac{1}{20}+\tfrac{1}{20}\beta\right)\left[\left(\tfrac{1}{12}+\tfrac{1}{10}\alpha\right)\rho_1 + \left(\tfrac{1}{4}+\tfrac{3}{20}\alpha\right)\rho_3\right] + \\
& + \left(\tfrac{1}{5}+\tfrac{1}{10}\beta\right)\left[\left(\tfrac{1}{4}+\tfrac{3}{20}\alpha\right)\rho_4 + \left(\tfrac{1}{12}+\tfrac{1}{10}\alpha\right)\rho_2\right] - \\
& - \left(\tfrac{1}{20}+\tfrac{1}{20}\beta\right)\left[\left(\tfrac{1}{4}-\tfrac{3}{20}\alpha\right)\rho_3 + \left(\tfrac{1}{12}-\tfrac{1}{10}\alpha\right)\rho_5\right] - \\
& - \left(\tfrac{1}{8}+\tfrac{1}{10}\beta\right)\left[\left(\tfrac{1}{12}-\tfrac{1}{10}\alpha\right)\rho_6 + \left(\tfrac{1}{4}-\tfrac{3}{20}\alpha\right)\rho_4\right] \Big\} + \ldots
\end{aligned}
\tag{4.2-9}
$$

The cross winding effect can be seen by comparing the terms above for flow in the x direction only. For $\beta \neq 0$, the terms provide unequal contribution to the v_{x_3} and v_{x_4} equations. A one row strip of two-dimensional elements cannot solve a one-dimensional problem accurately unless $\beta = 0$.

To further illustrate the convected inertia terms in the typical equation, selected terms from the v_{y_3} equation will be presented. The particular terms involving the y velocities are given, followed by simplifications to clarify their meaning.

Let all nodal values of the density take on the uniform value ρ_0. First consider $\alpha = \beta = 0$, or no upwind weighting. With these simplifications, the v_{y_3} terms reduce to

$$\frac{2\rho_0}{144}\{(2v_{y_1}+v_{y_2}+3v_{y_3})(v_{y_2}-v_{y_1})+(v_{y_1}+2v_{y_2}-12v_{y_3}-6v_{y_4}+ +v_{y_5}+2v_{y_6})(v_{y_4}-v_{y_3})+(3v_{y_3}+2v_{y_5}+v_{y_6})(v_{y_6}-v_{y_5})\} \tag{4.2-10}$$

Notice that the appearance is that of weighted sums of the three available velocity gradients.

Letting $\beta = 1$ and $\alpha = 0$ corresponds to a dominant y velocity across the element row. The terms then reduce to

$$\frac{4\rho_0}{144}\{(v_{y_1}-v_{y_2}+v_{y_3}-v_{y_4})(v_{y_2}-v_{y_1})+(v_{y_1}-v_{y_2}+6v_{y_3}-6v_{y_4}+ +v_{y_5}-v_{y_6})(v_{y_4}-v_{y_3})+(V_{y_3}-v_{y_4}+v_{y_5}-v_{y_6})(v_{y_6}-v_{y_5})\} \tag{4.2-11}$$

Although the form of weighted sums of velocity gradients can still be seen, the weights have changed. Terms on the upwind row, $v_{y_1}, v_{y_3}, v_{y_5}$, are slightly increased, while

terms on the downwind row, $v_{y_2}, v_{y_4}, v_{y_6}$, are substantially reduced.

Finally, consider $\alpha = \beta = 1$ or dominant velocities in the positive direction of each axis. The terms reduce to

$$\frac{\rho_0}{144}\{(14v_{y_1} - 14v_{y_2})(v_{y_2} - v_{y_1}) +$$

$$+(-22v_{y_1} + 22v_{y_2} - 30v_{y_4} - 2v_{y_5} + 2v_{y_6})(v_{y_4} - v_{y_3}) +$$

$$+ 28v_{y_3}v_{y_4} + (-4v_{y_5} + 4v_{y_6})(v_{y_6} - v_{y_5})\} \qquad (4.2\text{-}12)$$

Here the shift to upwind is less obvious.

Upwind Weighting on Terms other than Convected Inertias

In a consistent application of the present variational method, the same weighting functions are used in all terms of an equation. To assure stability, however, it appears necessary only to apply upwind weighting to the convected terms. In practice, nodal equations of elements without an upwind neighbor are ill-conditioned by the application of such weighting to the entire equation. This difficulty may be avoided by prescribing nodal values for upwind boundary nodes. Such artificial boundary conditions are not desired since it may be difficult to find appropriate values to prescribe prior to solution of the problem.

To illustrate this, elements of the density rate matrix $[RM]_e$ will be presented, where

$$[RM]_e = \int_{V_{F_e}} [L^*]^T [L] \, dV \qquad (4.2\text{-}13)$$

Using the bilinear interpolation functions for [L] and the upwinded weighting functions for $[L^*]$, the elements of the first row are

$$\begin{aligned} RM(1,1) &= (\tfrac{1}{3} - \tfrac{1}{4}\alpha)(\tfrac{1}{3} - \tfrac{1}{4}\beta) \\ RM(1,2) &= (\tfrac{1}{6} - \tfrac{1}{4}\alpha)(\tfrac{1}{3} - \tfrac{1}{4}\beta) \\ RM(1,3) &= (\tfrac{1}{6} - \tfrac{1}{4}\alpha)(\tfrac{1}{6} - \tfrac{1}{4}\beta) \\ RM(1,4) &= (\tfrac{1}{3} - \tfrac{1}{4}\alpha)(\tfrac{1}{6} - \tfrac{1}{4}\beta) \end{aligned} \qquad (4.2\text{-}14)$$

Consider the case of full α winding, and no β winding. Two of the terms become negative, while following a lumping procedure, the sum of these terms is zero. When assembled into a global matrix, there will be no nonzero terms added if there are no upwind neighbors.

The momentum rate or mass matrix behaves similarly. This matrix is

$$[VM]_e = \int_{V_{F_e}} [N^*]^T [N] [L] \{\rho\} \, dV \qquad (4.2\text{-}15)$$

Using the bilinear functions for [N] and [L], and the winded functions for $[N^*]$, the lumped mass is

$$VM(1,1) = -\frac{1}{360}\rho \qquad (4.2\text{-}16)$$

where ρ is an assumed uniform value of the density, and $\alpha = 1$, $\beta = 0$. For comparison, the result with no winding and uniform density is $\frac{1}{4}\rho$ for the lumped mass.

4.3 Discretization of the Elastic Solid Functional

Membrane Element

The elemental contributions arising from the partial differentiation of the leading term in the solid functional with respect to the nodal values of the adjoint displacement will be called the element restoring forces. This membrane element will have structural displacements that are linear combinations of the two sets of nodal values, i.e.,

$$\begin{Bmatrix} u_x \\ u_y \end{Bmatrix} = \begin{bmatrix} N_1 & 0 & N_2 & 0 \\ 0 & N_1 & 0 & N_2 \end{bmatrix} \begin{Bmatrix} u_{x_1} \\ u_{y_1} \\ u_{x_2} \\ u_{y_2} \end{Bmatrix} \qquad (4.3\text{-}1)$$

The adjoint variables will be interpolated similarly.

Evaluating the strains and assuming a linear elastic material, the stresses are found to be

$$s_{xx} = Ee_{xx}$$

$$s_{xy} = s_{yx} = 2Ge_{xy}$$

$$s_{yy} = 0 \qquad (4.3\text{-}2)$$

The leading term in the element functional is found, after insertion of the preceding, to be

$$I_e = \int_{t_1}^{t_2} \int_{V_{S_\epsilon}} \left\{ u^*_{x,x} S_{xx}(1 + u_{x,x}) + u^*_{y,x} S_{xx} u_{y,x} + u^*_{y,x} S_{x,y} \right\} dV\, dt$$

$$= \int_{t_1}^{t_2} \int_{0}^{L} \left\{ (u^*_{x_1} N^*_{1,x} + u^*_{x_2} N^*_{2,x}) S_{xx}(1 + u_{x,x}) + \right.$$

$$\left. + (u^*_{y_1} N^*_{1,x} + u^*_{y_2} N^*_{2,x})(S_{xx} u_{y,x} + S_{xy}) \right\} h\, dl \qquad (4.3\text{-}3)$$

The element restoring forces are

$$\frac{\partial I_e}{\partial u^*_{x_1}} = Q_{x_1} = \int_0^L \left\{ N^*_{1,x} hE\left(u_{x,x} + \tfrac{1}{2} u^2_{x,x} + \tfrac{1}{2} u^2_{y,x} + \right.\right.$$

$$\left. \left. + N^*_{1,x} hE\left(u^2_{x,x} + \tfrac{1}{2} u^3_{x,x} + \tfrac{1}{2} u^2_{y,x} u_{x,x}\right) \right\} dl \qquad (4.3\text{-}4a)$$

$$\frac{\partial I_e}{\partial u^*_{y_1}} = Q_{y_1} = \int_0^L \left\{ N^*_{1,x}\ hG u_{y,x} + N^*_{1,x} hE\left(u_{x,x} u_{y,x} + \right.\right.$$

$$\left. \left. + \tfrac{1}{2} u^2_{x,x} u_{y,x} + \tfrac{1}{2} u^3_{y,x}\right) \right\} dl \qquad (4.3\text{-}4b)$$

$$\frac{\partial I_e}{\partial u^*_{x_2}} = Q_{x_2} = \int_0^L \Big\{ N^*_{2,x}\, hE\Big(u_{x,x} + \tfrac{1}{2}u^2_{x,x} + \tfrac{1}{2}u^2_{y,x}\Big) + N^*_{2,x}\, hE\Big(u^2_{x,x} + \tfrac{1}{2}u^3_{x,x} + \tfrac{1}{2}u^2_{y,x}u_{x,x}\Big)\Big\}\, d\ell \qquad (4.3\text{-}4c)$$

$$\frac{\partial I_e}{\partial u^*_{y_2}} = Q_{y_2} = \int_0^L \Big\{ N^*_{2,x}\, hG\, u_{y,x} + N^*_{2,x}\, hE\Big(u_{x,x}u_{y,x} + \tfrac{1}{2}u^2_{x,x}u_{y,x} + \tfrac{1}{2}u^3_{y,x}\Big)\Big\}\, d\ell \qquad (4.3\text{-}4d)$$

These results are identical to those obtained by retaining all terms in the virtual work equations for large deformations. To reach the simplified form usually used in practice, the assumptions required are

1. $1 + u_{x,x} \doteq 1$
2. $\frac{1}{2}u^2_{x,x} << u_{x,x}$
3. $s_{xy} = 0$ but $u_{y,x} \neq 0$

These assumptions are consistent with the practice of neglecting higher powers of small terms.

4.4 Fluid Structure Interface

Typical Nodal Equation on the Interface

The condition on the interface S_I of the fluid region V_F and the structural region V_S is continuity of velocity and temperature. For the specific case of inviscid flow, this is reduced to continuity of the normal velocity. In practice, this means the equation for the normal velocity of a node on the interface will contain contributions from elements in both regions.

The example presented here is the momentum equation for a node common to two unit square fluid elements and two membrane elements (Fig. 4.3). This equation will contain convected inertia and pressure terms from the fluid element and restoring forces from the membrane. In addition, the nodal mass will be the sum of lumped masses from the fluid and membrane elements.

The equation for the y velocity at node 3 will be presented. An external pressure of magnitude $\hat{p}$ will be applied to the membrane. Each membrane element will have a thickness h and uniform density ρ_S. In this example, contributions from the x velocities to the convected inertias will be neglected. The fluid will have a uniform density ρ_F and pressure p_0. These conditions are appropriate for initial motion of the membrane into stationary fluid.

Some contributions to the equation for v_{y_3} are:

structural mass = $\frac{1}{2}\rho_S h1 + \frac{1}{2}\rho_S h1 = \rho_S h$

fluid lumped mass = $\frac{1}{18}\rho_1 + \frac{1}{36}\rho_2 + \frac{2}{9}\rho_3 + \frac{1}{9}\rho_4 +$

$+ \frac{1}{18}\rho_5 + \frac{1}{36}\rho_6 = \frac{1}{2}\rho_F$

pressure gradient = $-\frac{1}{12}p_1 - \frac{1}{12}p_2 - \frac{1}{3}p_3 - \frac{1}{3}p_4 -$

$- \frac{1}{12}p_5 - \frac{1}{12}p_6 = -p_0$

external pressure = $-\frac{1}{6}1\hat{p}_1 - \frac{2}{3}1\hat{p}_3 - \frac{1}{6}1\hat{p}_5 = -\hat{p}$

Let $\alpha = 0$, $\beta = 1$, and Q_{y_3} be the string restoring force. The equation for v_{y_3} is

$$(\rho_S h + \tfrac{1}{2}\rho_F)\dot{v}_{y_3} = -Q_{y_3} - p_0 + \hat{p} -$$

$$- \frac{\rho_F}{36}\left[(v_{y_1} - v_{y_2} + v_{y_3} - v_{y_4})(v_{y_2} - v_{y_1}) + (v_{y_1} - v_{y_2} + 6v_{y_3} - \right.$$

$$\left. - 6v_{y_4} + v_{y_5} - v_{y_6})(v_{y_4} - v_{y_3}) + (v_{y_3} - v_{y_4} + v_{y_5} - v_{y_6})(v_{y_6} - v_{y_5})\right] \quad (4.4\text{-}1)$$

If $\hat{p}$ has the value of the rest pressure of the fluid, there is no pressure gradient across the membrane. If the fluid velocities away from the membrane can be neglected, the equation simplifies to

$$(\rho_S h + \tfrac{1}{2}\rho_F)\dot{v}_{y_3} = -Q_{y_3} - \frac{\rho_F}{36}\left[(v_{y_1} + v_{y_3})^2 + 2v_{y_3}^2 + (v_{y_3} + v_{y_5})^2\right] \quad (4.4\text{-}2)$$

Continuity on the Interface

The only condition on admissible trial functions on the interface surface S_I is that the velocity and temperature fields be continuous. Continuity of trial functions is a common requirement in finite element procedures and is generally met by requiring elements to be compatible. The following will investigate the compatibility of a structural element and a fluid element.

To facilitate this, consider the mesh segment shown in Fig. 4.4. The elements 2,3,4 and 8 are fluid elements, elements 1,5,6 and 7 are structural elements, and nodes 1,5 and 9 are the interface surface nodes. Let u_α represent the structural displacements, v_α be the fluid velocities, N_i^e be the interpolation function for node i in element e, and $N_{i_S}^e$ denote that function restricted to the interface. The triangular elements will allow linear variation in the variable fields and this will be assumed for both regions. Let $u_{\alpha_S}^e$ be the function u_α restricted to element e on surface S_I.

Then in element 8, a fluid element, the velocity is

$$v_\alpha = \sum_i N_i^8 v_{\alpha_i} \qquad i = 5,6,9$$

$$= N_5^8 v_{\alpha_5} + N_6^8 v_{\alpha_6} + N_9^8 v_{\alpha_9} \qquad (4.4\text{-}3)$$

If $N_{6_S}^8 = 0$ as is common, the velocity on S_I is

$$v_{\alpha_S}^8 = N_{5_S}^8 v_{\alpha_5} + N_{9_S}^8 v_{\alpha_9} \qquad (4.4\text{-}4)$$

In a similar manner, the temperature is

$$T_S^8 = M_{5_S}^8 T_5 + M_{9_S}^8 T_9 \qquad (4.4\text{-}5)$$

In element 7, a structural element, the displacement is

$$u_\alpha^7 = N_5^7 u_{\alpha_5} + N_8^7 u_{\alpha_8} + N_9^7 u_{\alpha_9} \qquad (4.4\text{-}6)$$

Then, on S_I, the displacement becomes

$$u_{\alpha_S}^7 = N_{5_S}^7 u_{\alpha_5} + N_9^7 u_{\alpha_9} \qquad (4.4\text{-}7)$$

if

$$N_{8_S}^7 = 0$$

and the temperature is

$$T_S^7 = M_{5_S}^7 T_5 + M_{9_S}^7 T_9 \qquad (4.4\text{-}8)$$

Since $N_i^e = 0$ at node $j \neq i$ and $N_i^e = 1$ for node i, at node 5, the interface values of the field variables are

$$v_{\alpha_S}^8 = v_{\alpha_5}$$
$$T_S^8 = T_5 \qquad (4.4\text{-}9)$$

and

$$u_{\alpha_S}^7 = u_{\alpha_5}$$
$$T_S^7 = T_5 \qquad (4.4\text{-}10)$$

Since the interpolation functions are not time dependent, the structural velocity is

$$\dot{u}_\alpha = \sum_i N_i^e \dot{u}_{\alpha_i} \qquad \text{for } i \text{ in } e \qquad (4.4\text{-}11)$$

Then at the nodes, the velocity and temperature are continuous and equal to the nodal value.

The continuity along the interface from node 5 to node 9 is expressed as

$$\begin{aligned} v_{\alpha_S}^8 &= \dot{u}_{\alpha_S}^7 \\ T_S^8 &= T_S^7 \end{aligned} \qquad (4.4\text{-}12)$$

or

$$N_{5_S}^8 v_{\alpha_5} + N_{9_S}^8 v_{\alpha_9} = N_{5_S}^7 \dot{u}_{\alpha_5} + N_{9_S}^7 \dot{u}_{\alpha_9}$$

$$M_{5_S}^8 T_5 + M_{9_S}^8 T_9 = M_{5_S}^7 T_5 + M_{9_S}^7 T_9 \qquad (4.4\text{-}13)$$

This can only hold for arbitrary values of the nodal parameters if the interpolation functions on the interface are such that

$$\begin{aligned} N_{5_S}^8 &= N_{5_S}^7 \\ N_{9_S}^8 &= N_{9_S}^7 \\ M_{5_S}^8 &= M_{5_S}^7 \\ M_{9_S}^8 &= M_{9_S}^7 \end{aligned} \qquad (4.4\text{-}14)$$

This is the usual requirement for compatibility of elements.

4.5 Time Integration

The actual form of the matrix equations is an integral over time, e.g.,

$$\frac{\partial I}{\partial \{v^*\}} = \int_{t_1}^{t_2} \left[[VM] \{\dot{v}\} + [VV] \{v\} - \{P\} \right] dt = 0 \qquad (4.5\text{-}1)$$

This integral equation is satisfied in practice by solving the ordinary differential equation obtained by setting the integrand to zero for all time.

For reasons of simplicity in implementation, a Runge-Kutta integration package was used. This routine calculates end of time step values based upon a weighted average of the rates obtained from four evaluations during the step.

Although this is a highly nonlinear equation set, the time step criterion for linear problems has proven adequate. Specifically, the time step is chosen such that information propagating at the local speed of sound travels no farther than one element width in one time step. In practice, one sound speed is chosen, usually the rest speed of sound. The maximum time step is calculated based upon the smallest element in the field. Since local sound speeds may rise considerably above the rest value, the calculated time step is halved. Parametric studies of numerical solutions have shown this to be adequate.

5. NUMERICAL EXAMPLES

Several numerical problems are presented. Their purpose is to exercise the major capabilities of the variational formulation and its computer implementation. Since a combined problem with compressible isentropic fluid and a large deformation structure is quite complex, simpler examples are given first. Understanding of these simple examples was essential to adequately solve the combined problem.

To verify the fluid element used in the present method, problems of a one-dimensional wave tube have been solved. This problem can demonstrate extreme fluid motions for which a limited analytical solution is available.

The wave tube is enlarged to two dimensions by examining a radially expanding cylinder in an infinite fluid. Valuable insight into the functioning of the upwind weighting is obtained here.

The final example is transient motion of a membrane with fluid on one side. In the first of two cases considered, initial motion of the membrane disturbs the fluid. In the second, a pressure wave traverses the fluid and excites the membrane.

5.1 Piston Wave Tube

The one-dimensional gas dynamics of a rigid piston moving in a tube filled with a perfect gas was investigated. The pressure and velocity of the inviscid gas were calculated using a prescribed motion of the piston. The movement of the piston is modeled by changing the coordinates and velocities of the nodes assigned to the piston surface. When the element in front of the piston is reduced to a certain size, it is eliminated from the problem solution.

The rest speed of sound for the following examples is 1000 fps. In the first example, the piston is started impulsively with a speed of 500 fps and keeps this speed for all time. In the second example, the piston velocity increases linearly from rest to 500 fps at .002 sec, then decreases linearly to rest at .004 sec. The parameter α is the upwind weight in the direction of motion. With one exception which will be noted, symmetric weighting was used in the transverse direction. The time step was half the linear stability limit based upon the rest speed of sound and the initial configuration mesh size.

Figure 5.1 presents the fluid velocity and pressure for the constant speed piston. The calculated pressure ratio across the shock agrees to less than 1% with that

given by the Rankine-Hugoniot relations (Liepman, Roshko, 1957). The smearing of the shock discontinuity is typical of the finite element solutions. There appears to be very little ringing or oscillation in the solution behind the shock.

The results for the second piston example are presented in Fig. 5.2. The example contains a compression wave which changes to a shock as well as an expansion wave. Also presented are some early time solutions by the method of characteristics for comparison. Agreement between the two is quite good in the expansion wave but due to smearing of the finite elements, agrees only fairly in the high gradient region of the shock front. Again there is little ringing near the peak, and the fluid behind the wave is reasonably still.

The deterioration of the solution as α is decreased to zero is presented in the next figure (Fig. 5.3). Deviations from the full upwind solution ($\alpha = 1.0$) are noticeable in the case of $\alpha = .5$. The solution for $\alpha = 0$ is barely recognizable. These results are consistent with those of Zienkiewicz (1977).

It is a characteristic of the present upwind weighting scheme that winding in one direction affects the solution in the other direction. An example of this is presented in Fig. 5.4. The calculated velocities for $\beta = \pm 1$ differ significantly from the $\beta = 0$ solution

of Fig. 5.2.

5.2. Cylindrical Wave

To demonstrate the two-dimensional capability of the present method, the piston problem was expanded to a cylindrical problem (Fig. 5.5). The goal is to calculate velocities and pressure in an initially still fluid surrounding an expanding cylinder. The cylinder radius and velocity are prescribed functions of time.

The initial radius of the cylinder is 1.0 ft. Its velocity increases linearly to 500 fps at .002 sec then decreases linearly to zero at .004 sec. The rest speed of sound is 1000 fps. The physical problem is in fact one-dimensional in the radius. A solution procedure using the method of characteristics is given by Rudinger (1969) but was not used because of its complexity.

Figure 5.5 also presents the calculated radial velocity and pressure. Since there should be no tangential velocity, the appropriate value of the tangential or cross wind weighting is zero. Table 5.1 shows the effect on the main flow caused by the inclusion of cross wind weighting. The local value of the winding parameter is

$$\beta = 1.0 \times \text{sign}\,(v_t)$$

The variation in the radial velocity and pressure are evidently associated with the fluctuating sign of the

very small tangential velocity.

5.3 Transient Motion of a Membrane

The most complex problem attempted was transient motion of a membrane wetted on one side by an inviscid compressible fluid. Such a problem exercises all the features of the computer program and illustrates the problems that can be attacked by the present method. The membrane is capable of accurately reproducing large motions and the fluid permits accurate and stable calculation of motion in the presence of extreme gradients. The problem at hand will illustrate the proper coupling of the two regions at their interface.

The membrane is stretched at $y = 0$ between $-2.5 \leq x \leq 2.5$ with rigid extensions to -5.0 and 7.5 in the x direction (Fig. 5.6). The fluid volume is truncated at $y = 5.0$ and extends from $x = -5.0$ to $x = 7.5$. The membrane starts with no deflection and an initial velocity such that a linear membrane in a vacuum would have a maximum deflection of 8% of its length. The fluid will start either at rest or have a uniform velocity in the x direction of magnitude $v_\infty = 1000$ fps or $M_\infty = .31$. The rest sound speed, a_0, is 3200 fps, and the rest pressure, p_0, is 2000 psf. The membrane has a small amplitude in vacuum natural frequency of 800 cps. A uniform pressure

of magnitude equal to the fluid rest pressure is applied to the outside of the membrane.

Table 5.2 presents variables at the membrane at a fixed time. The membrane has moved into the fluid to a point just short of its maximum. In all cases, the membrane is never affected by the presence or absence of the free stream velocity. The fluid velocity and pressure show a marked asymmetry when the cross wind is present. Apparently the asymmetric pressure gradient and x velocity are too small to affect the membrane motion in so short a time.

The physical properties of the present example of fluid and structure have been chosen such that the membrane is not appreciably affected by the presence of the fluid. For example, the period of oscillation is shortened by only a few percent, and the amplitude is not affected. Since the fluid has been truncated and a prescribed normal velocity imposed, reflections from these boundaries will lead to a solution that looks more like vibrations in a cavity at the later times. Some effects attributable to reflections can be seen in the results that follow.

Figure 5.7 presents pressure wave forms along the cavity center line. The times chosen correspond to quarter periods of the membrane motion. The disturbances appear to be large and the distortion in the wave shape

can be attributed to the changing local speed of sound. The amplitudes of the third cycle (compare $t = 2.76 \times 10^{-3}$ to $t = 1.50 \times 10^{-3}$ and $t = 0.30 \times 10^{-3}$) are noticeably larger than the first. This is probably due to the reflections off the boundary at $y = 5.0$.

Pressure wave forms on two planes parallel to the membrane show similar effects of reflections at later times (Fig. 5.8). In addition, results of a calculation with an initial velocity in the x direction of 1000 fps or $M_\infty = .31$ have been included. At all times presented, the waves have drifted noticeably downstream.

As a second case using the same model geometry, response of the membrane to a traveling pressure wave was considered. Both fluid and membrane are initially at rest and a step pressure increase from 2000 psf to 4000 psf is applied to the fluid boundary at $y = 5.0$. The wave propagates across the cavity and reflects off the membrane and its rigid extensions.

Three typical pressure wave forms on the cavity center line are presented in Fig. 5.9. The times chosen depict the incident wave, the time of maximum pressure and the wave as it returns to the $y = 5.0$ boundary. The motion of the center of the membrane is shown in Fig. 5.10. In Table 5.3 this same information is presented for comparison to a solution obtained by modal expansion. For the comparison solution, the motion of the membrane was calculated using the pressure at $y = 0$ as the forcing input.

LIST OF SYMBOLS

A free energy

C_v specific heat at constant volume

E internal energy of the fluid or Young's modulus

G shear modulus

I functional

L density interpolation function

M Mach number or temperature interpolation function

N nonlinear operator or velocity interpolation function

Q membrane restoring force

R gas constant

S entropy

T temperature

U internal energy of the solid

W weighting function

a local sound speed or acceleration vector

d spatial rate of strain tensor

e material strain tensor

f body force vector

g metric tensor

h membrane thickness or mesh spacing

k thermal conductivity

n surface normal

p pressure

q velocity magnitude or heat flux vector

r rate of heat generation or radial coordinate

s material stress tensor

u displacement

v velocity

α ξ or x direction winding parameter, $-1 \leq \alpha \leq 1$

β η or y direction winding parameter, $-1 \leq \beta \leq 1$

γ gas constant

δ Kronecker's delta

λ viscosity coefficient or Lamé constant

μ viscosity coefficient or Lamé constant

ξ coordinate of quadrilateral element

η coordinate of quadrilateral element

ρ density

ϕ velocity potential or direction in Fréchet differential

ψ direction in Fréchet differential

θ cylindrical coordinate angle

Superscripts and Subscripts

S solid

F fluid

$a,b,c,\ldots$ indices of material coordinates

e element quantity

r radial component

t tangential component

$\alpha,\beta,\gamma,\ldots$ indices of spatial coordinates

∞ far field value

f^* adjoint quantity f

$\hat{f}$ prescribed quantity f

Operators

∇f	gradient of f
$f_{,x}$	partial differentiation of f with respect to x
$f_{\|x}$	covariant differentiation of f with respect to x
$\frac{Df}{Dt}$	material derivative of f
$\dot{f}$	time derivative of f

LIST OF FIGURES

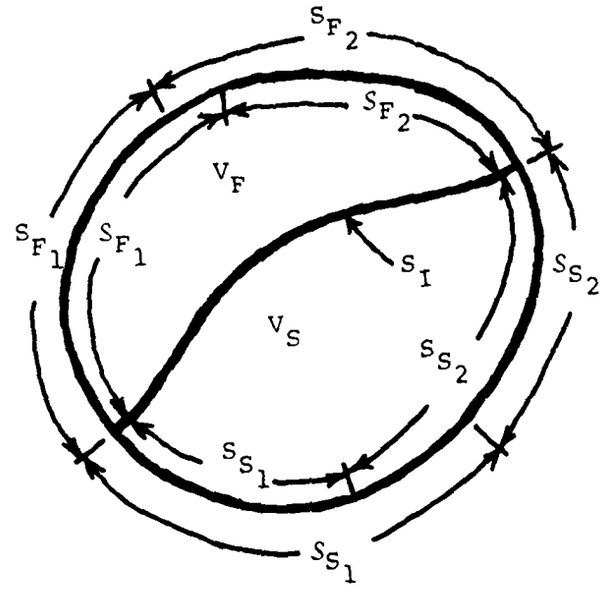

Fig. 3.1. Notation for fluid structure interaction principle.

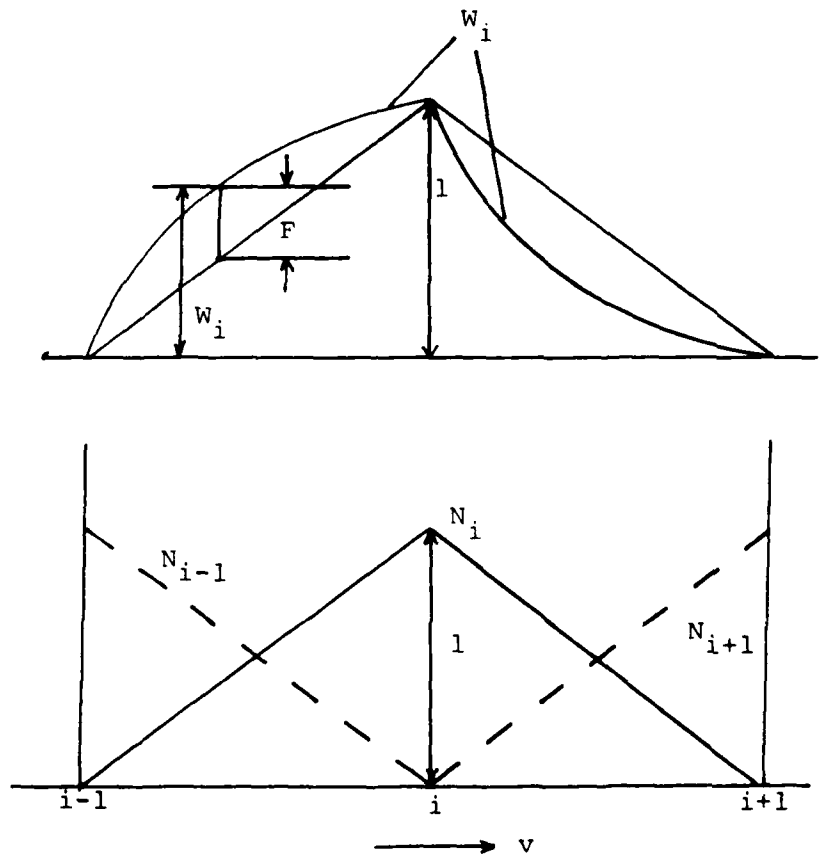

Fig. 4.1. Upwind weighted functions.

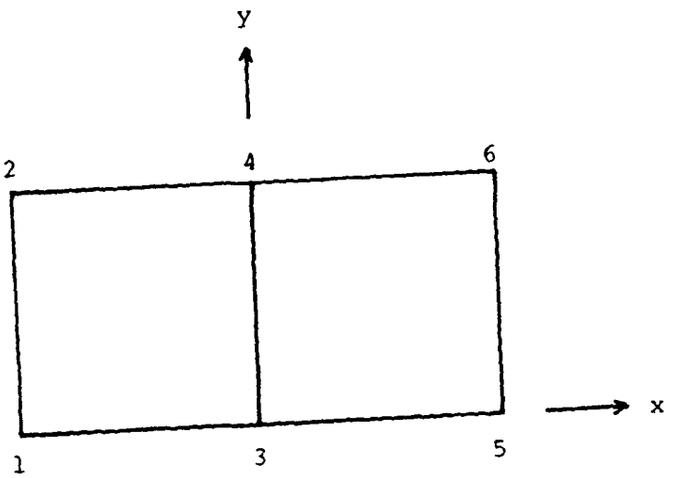

Fig. 4.2b. Mesh of square elements.

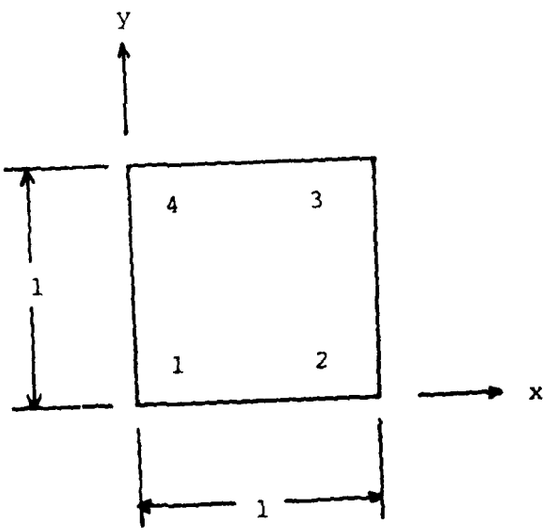

Fig. 4.2a. The unit square element.

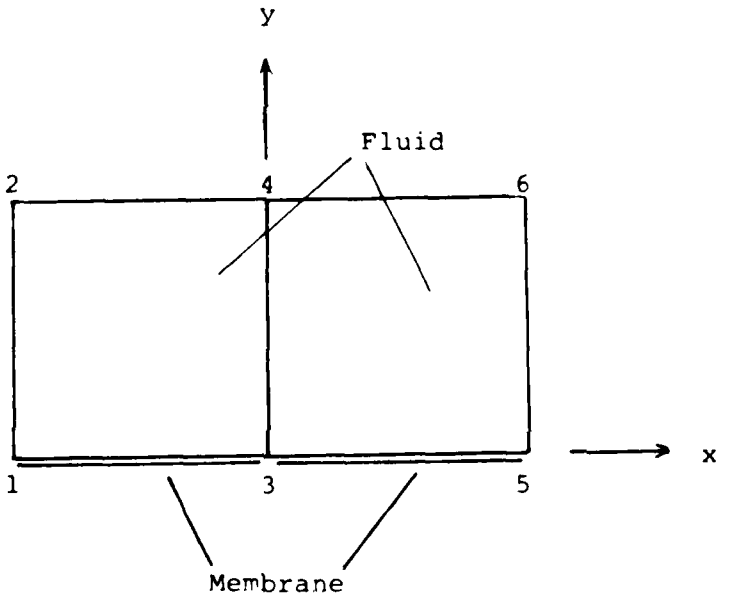

Fig. 4.3. Mesh of square and membrane elements.

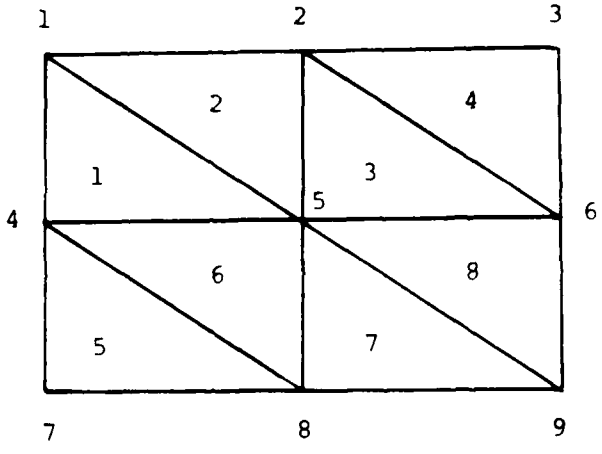

Fig. 4.4. Mesh for investigation of compatibility.

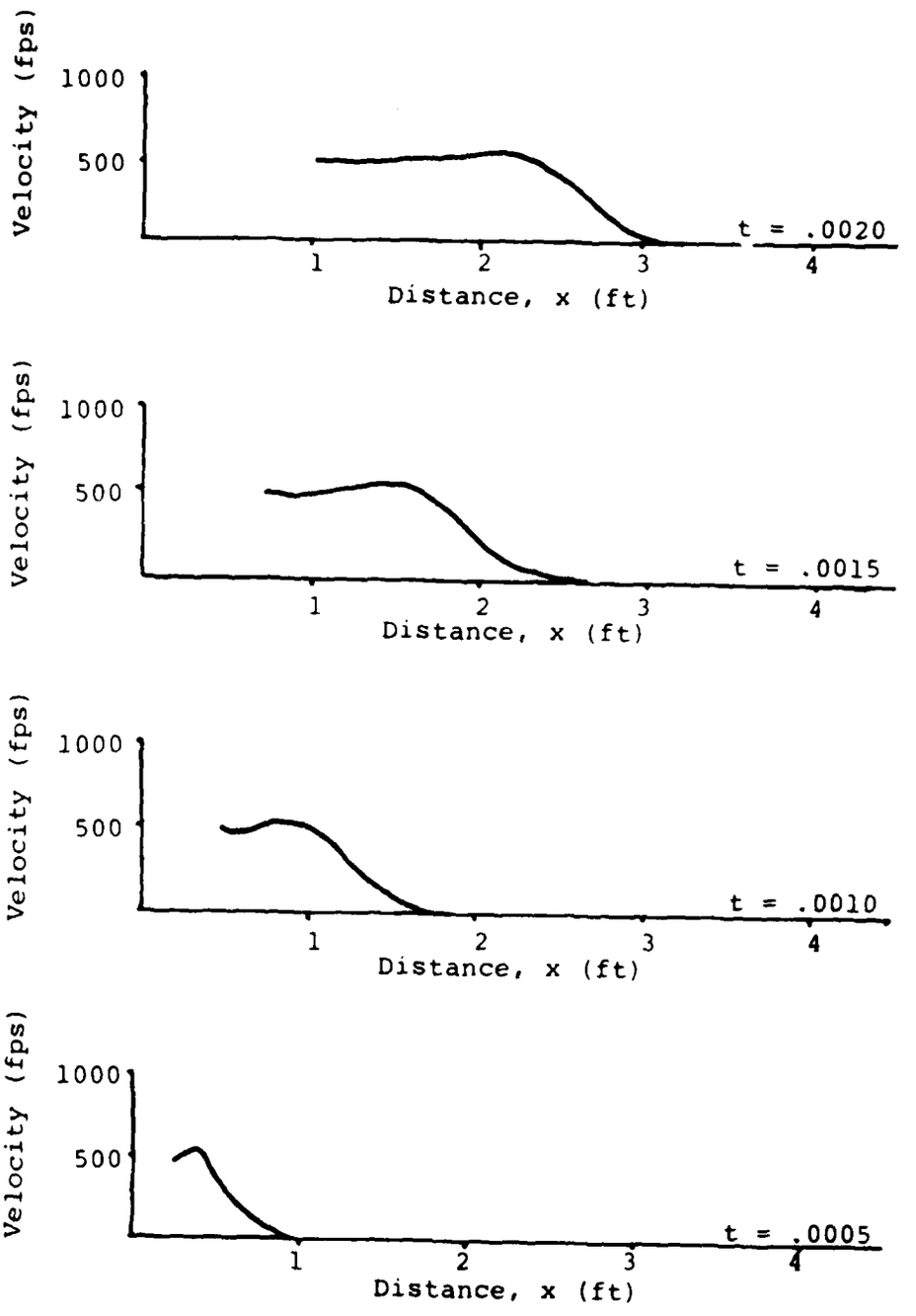

Note: rest speed of sound a_0 = 1000 fps

Fig. 5.1a. Constant speed piston - fluid velocity

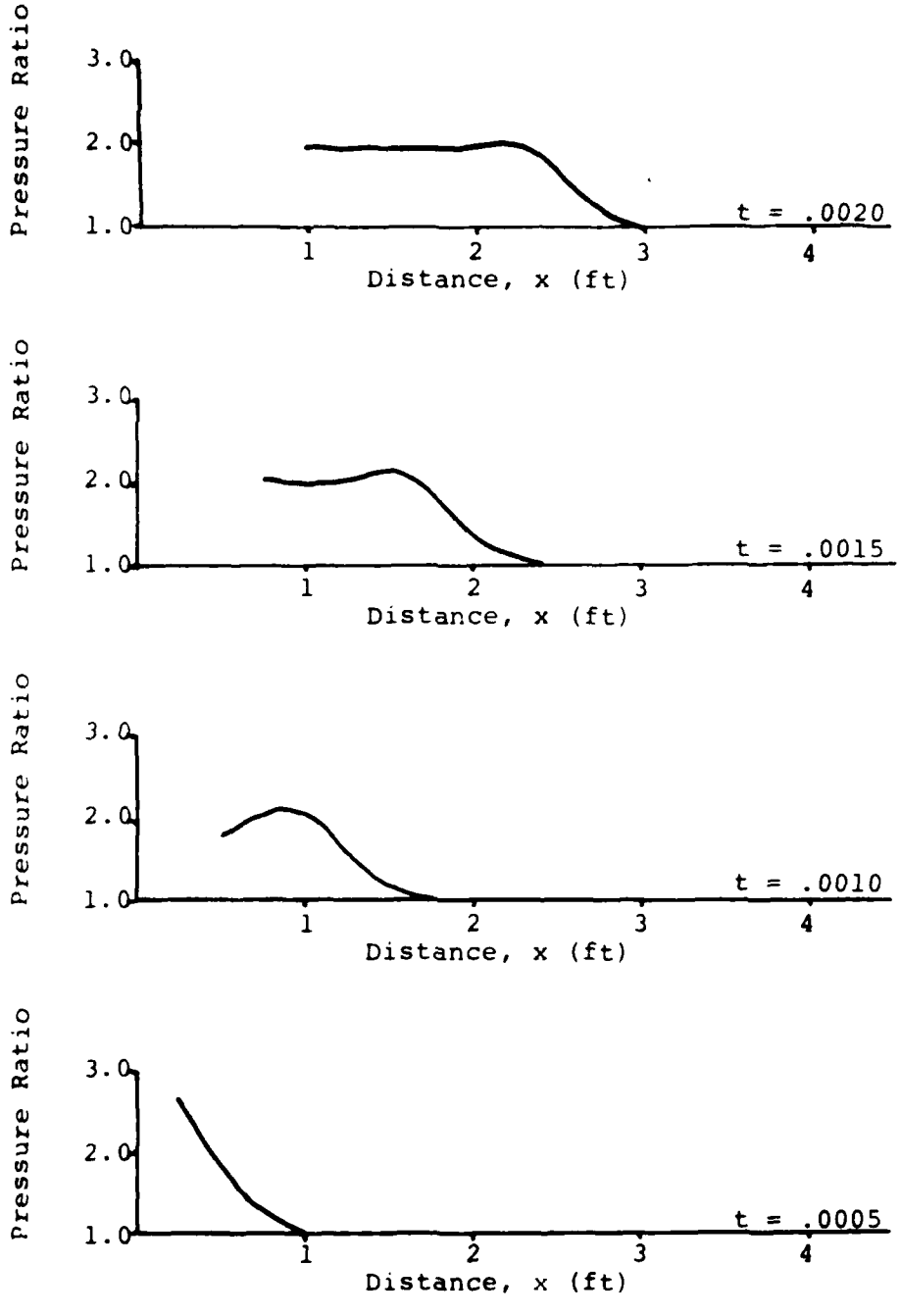

Note: pressure referenced to p_0 = 1700 psf

Fig. 5.1b. Constant speed piston - pressure ratio

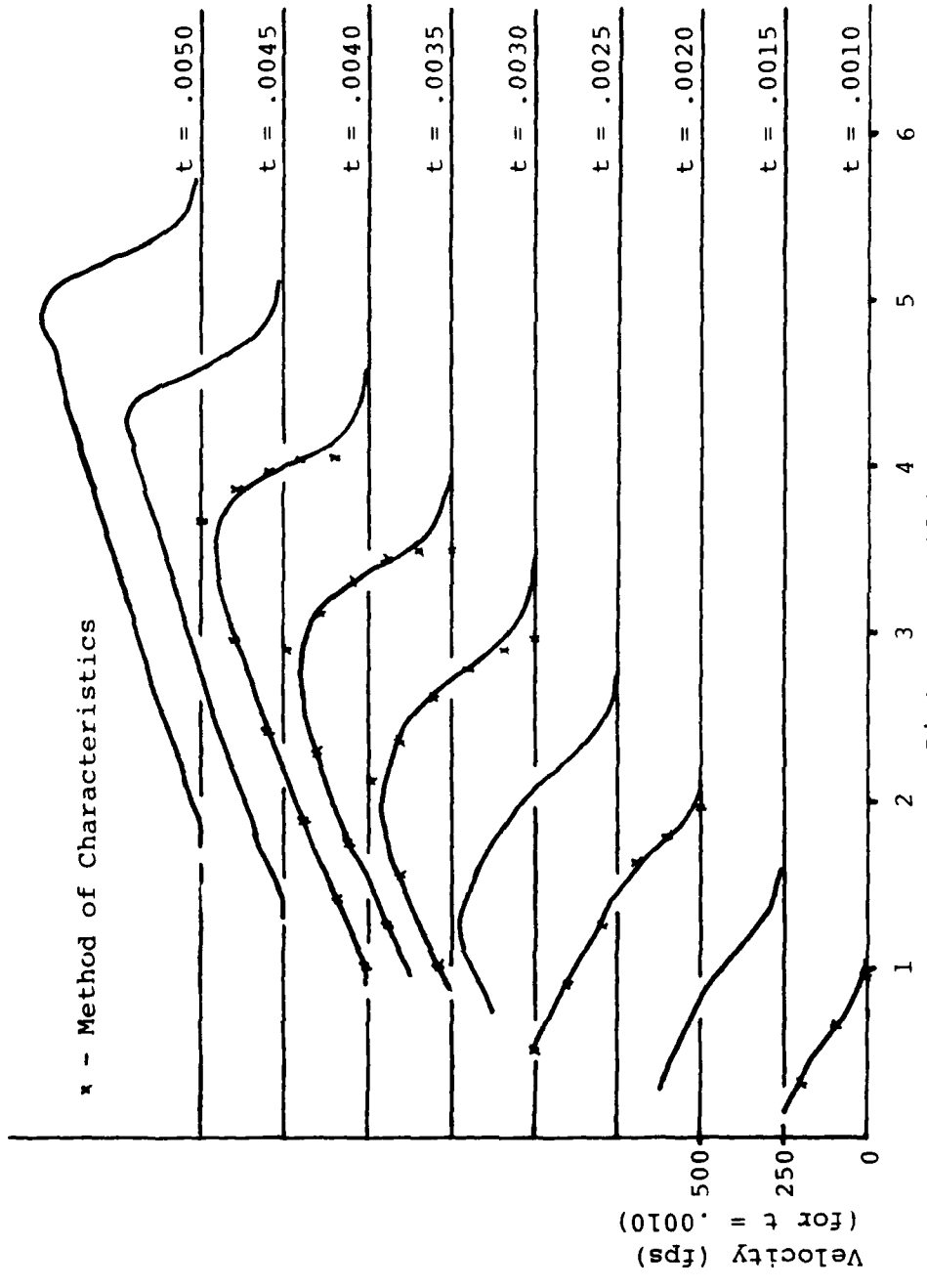

Fig. 5.2a. Piston wave tube - fluid velocity.

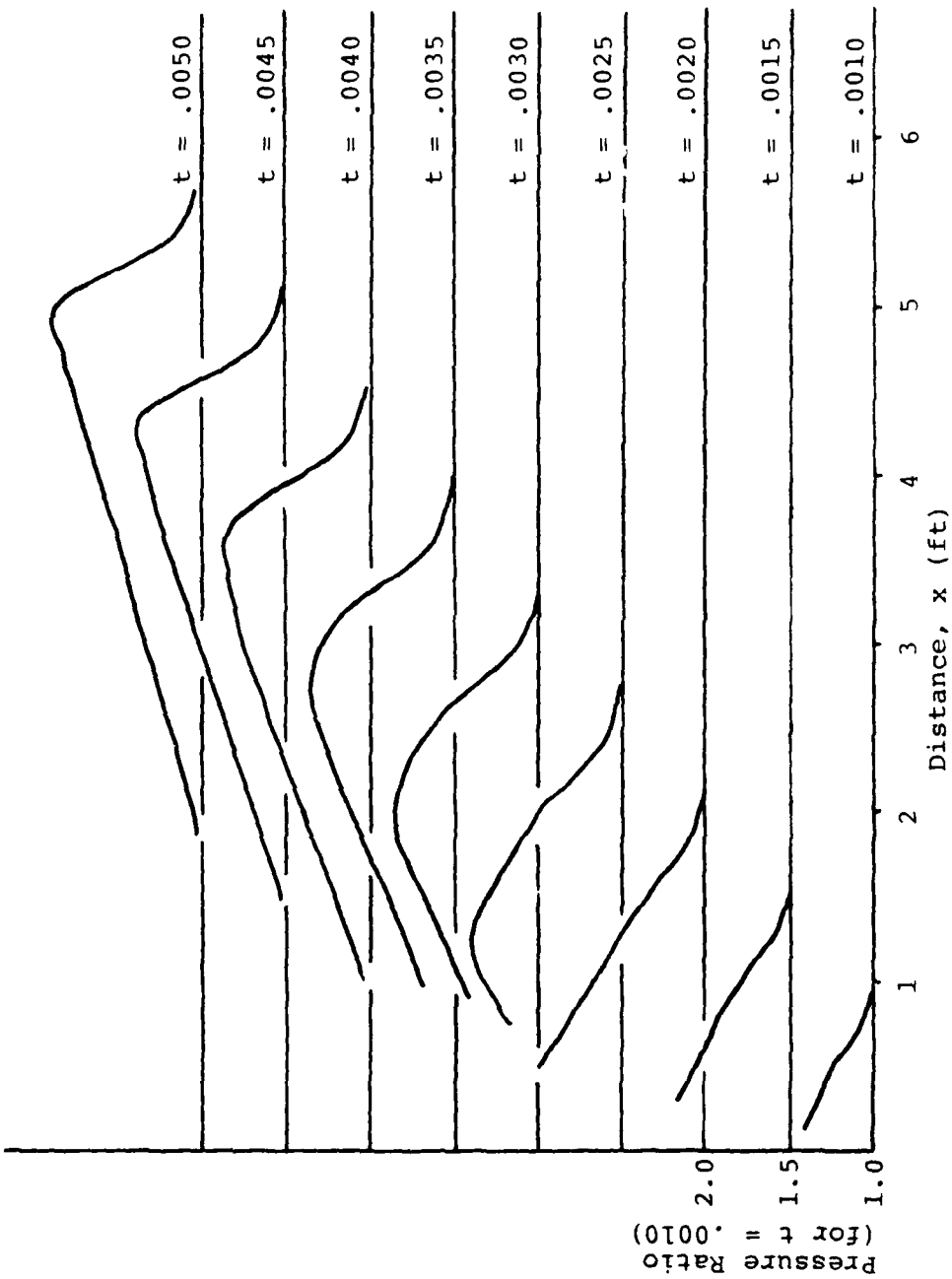

Fig. 5.2b. Piston wave tube - pressure ratio

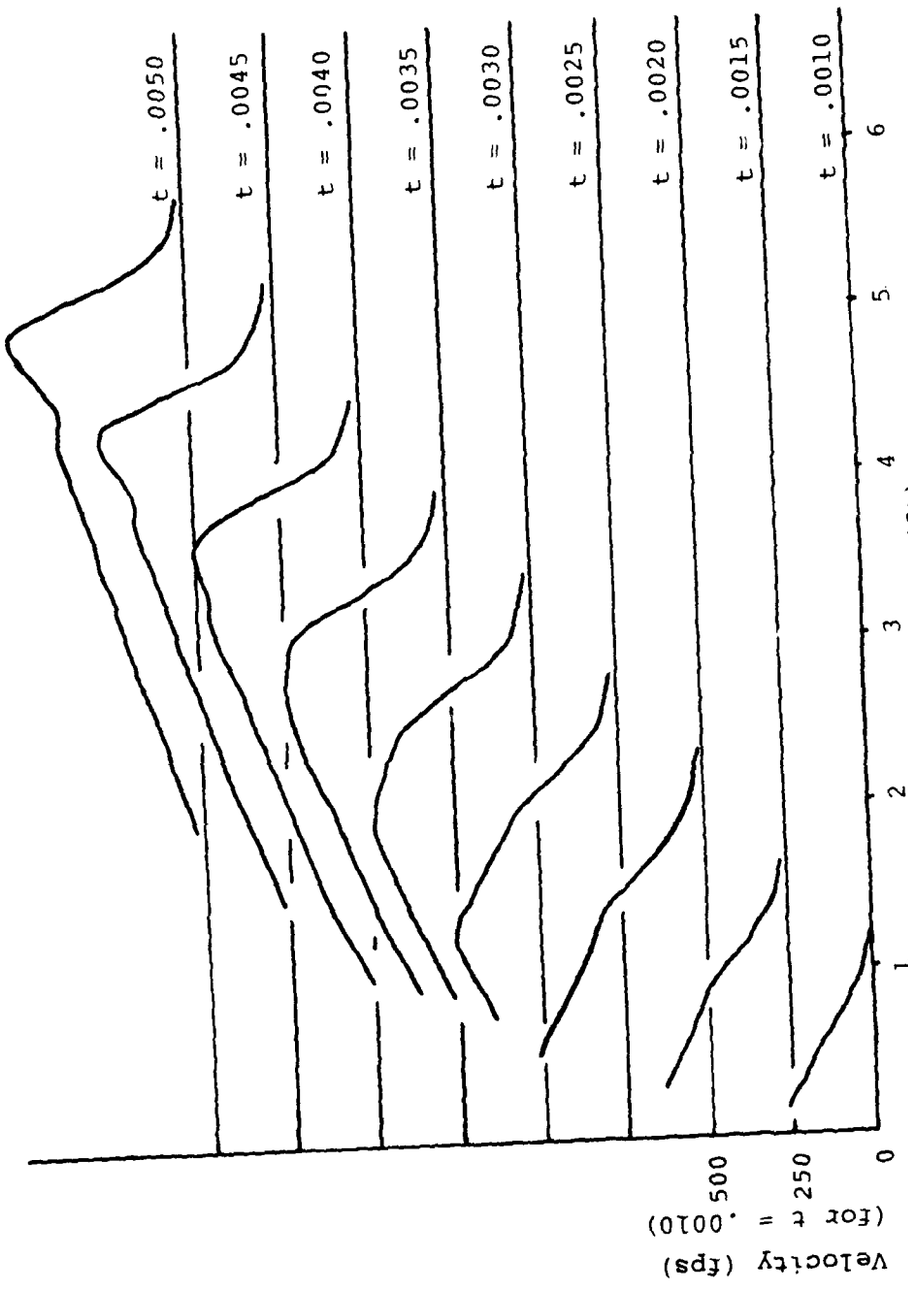

Fig. 5.3a. Piston wave tube - fluid velocity for $\alpha = .5$.

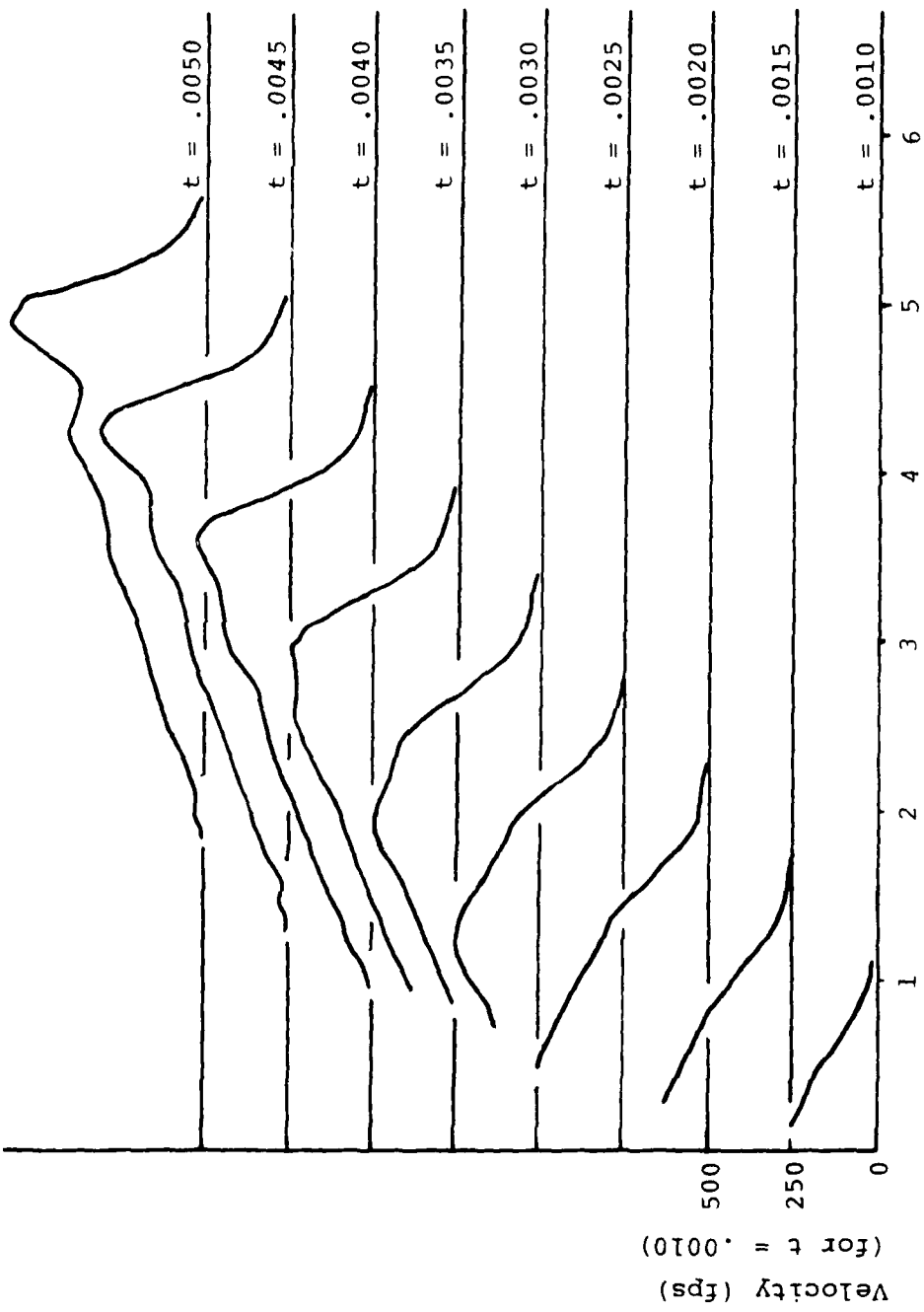

Fig. 5.3b. Piston wave tube - fluid velocity for α = .25.

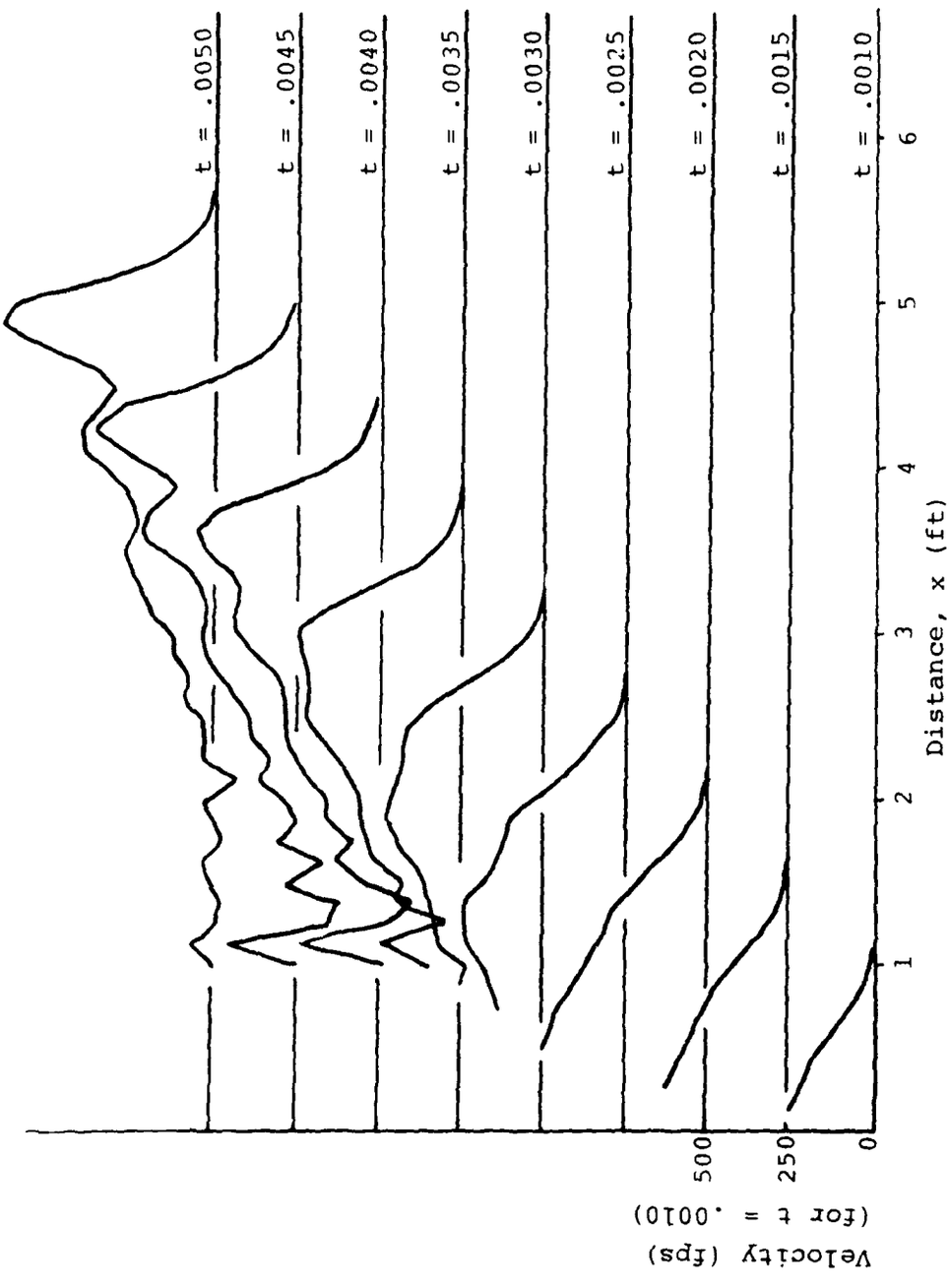

Fig. 5.3c. Piston wave tube - fluid velocity for $\alpha = 0$.

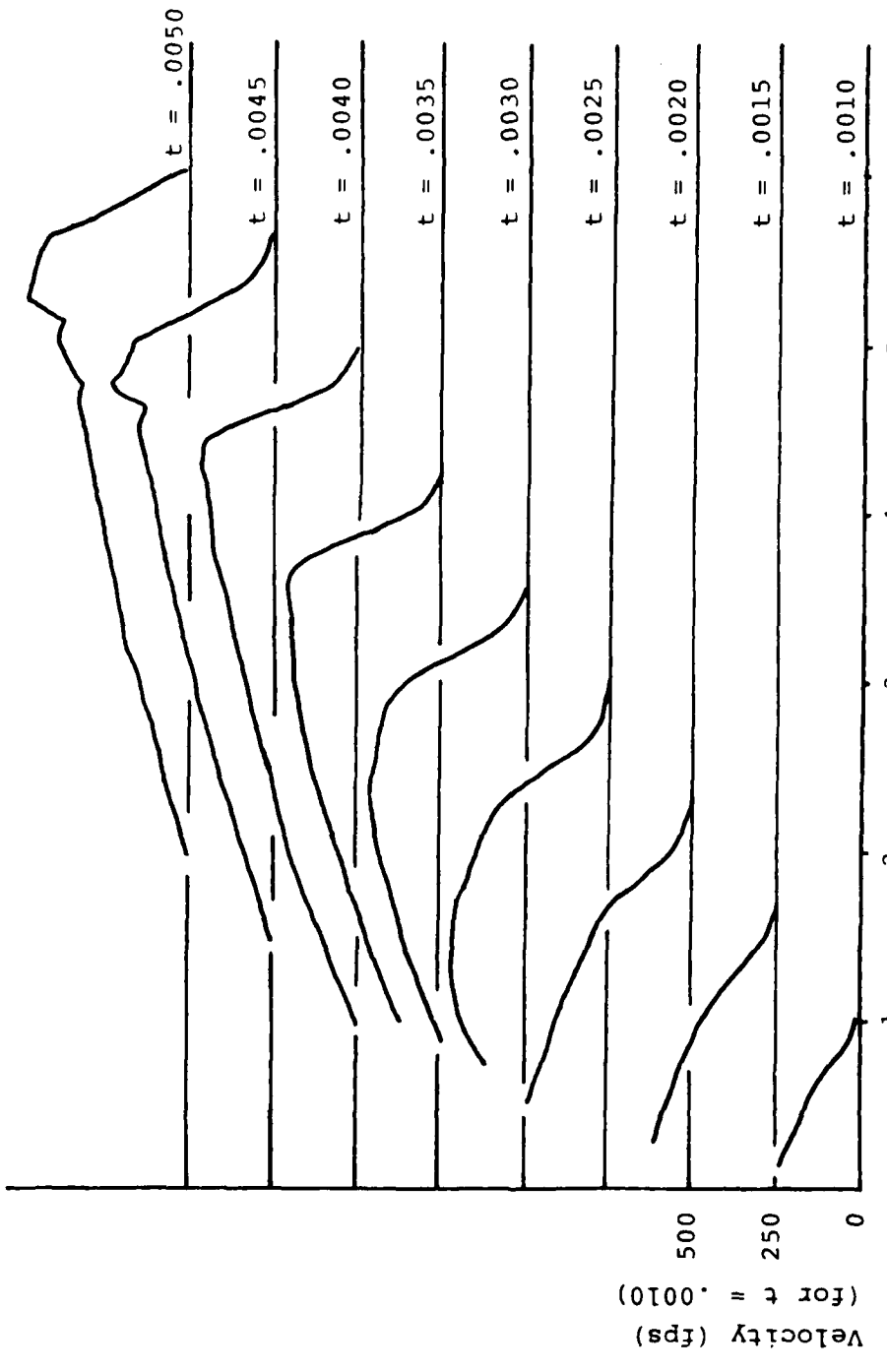

Fig. 5.4a. Piston wave tube - fluid velocity for $\beta = 1.0$.

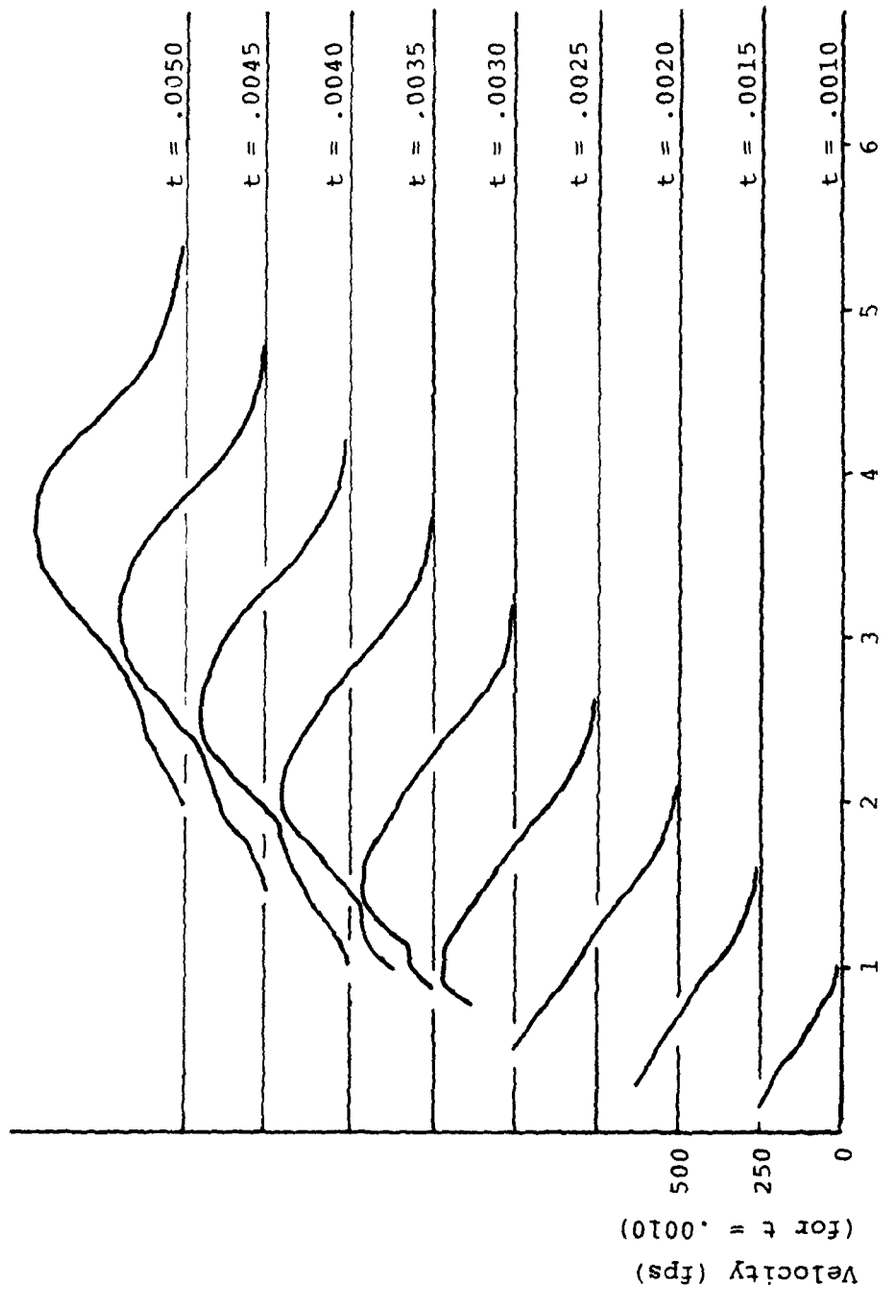

Fig. 5.4b. Piston wave tube - fluid velocity for $\beta = -1.0$.

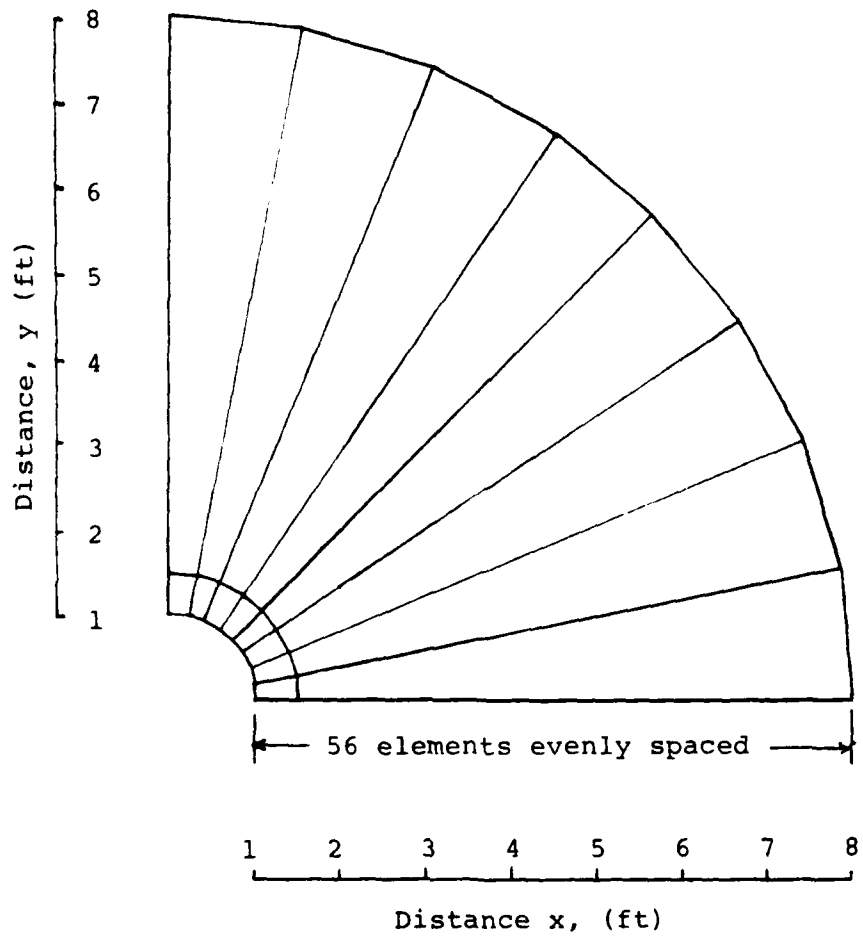

Fig 5.5a. Cylindrical wave - mesh.

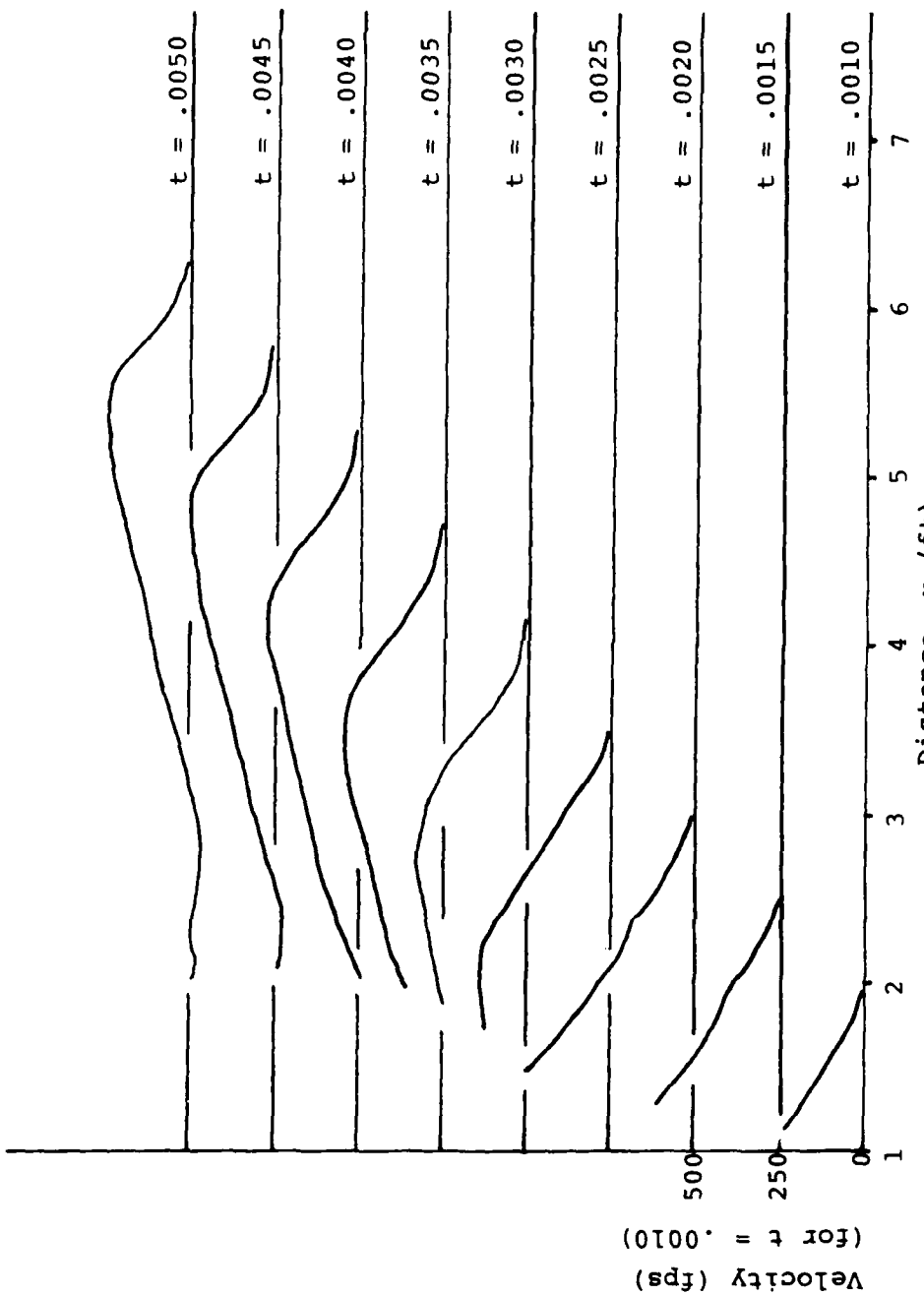

Fig. 5.5b. Cylindrical wave - radial velocity.

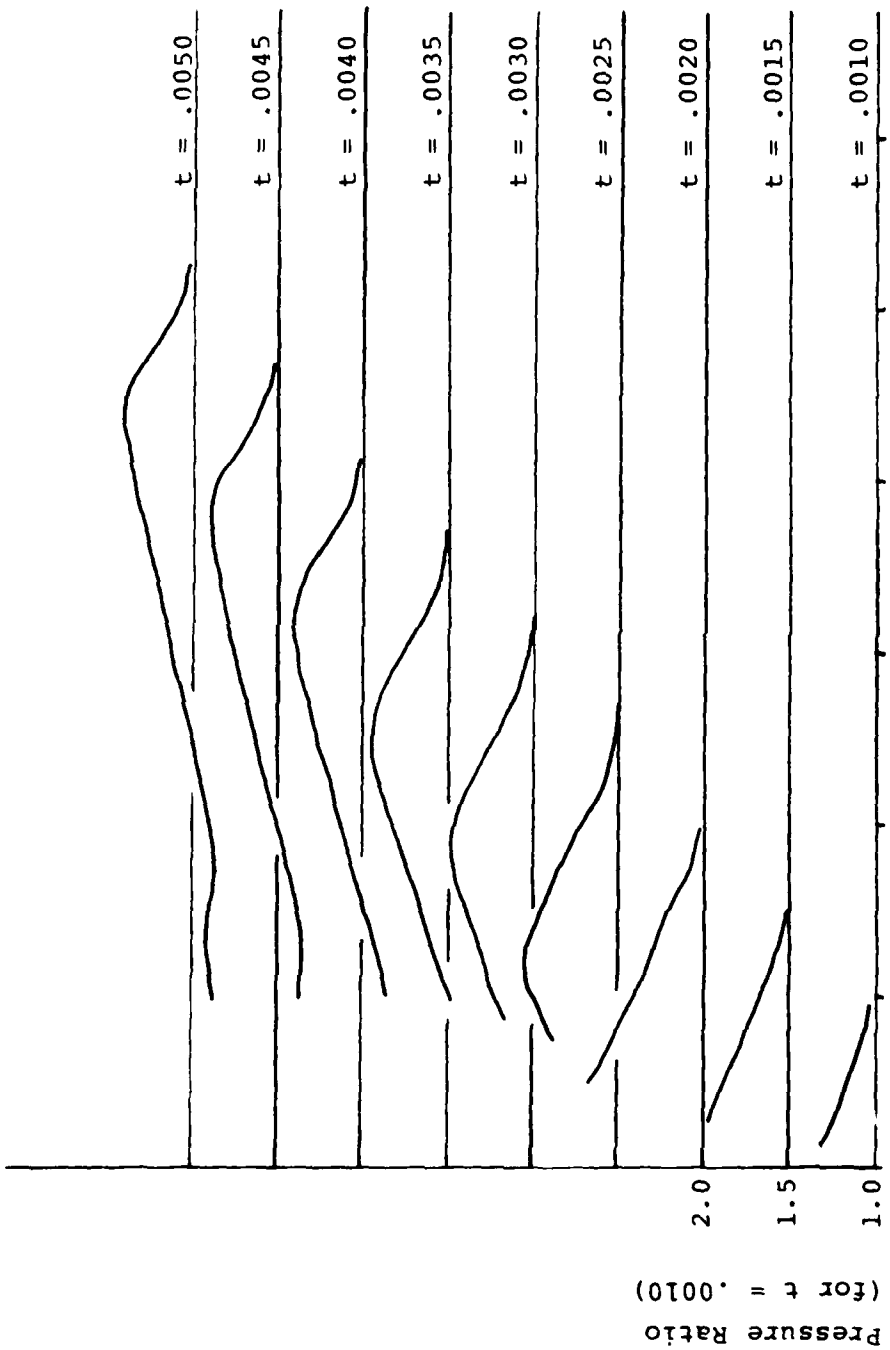

Fig. 5.5c. Cylindrical wave - pressure ratio.

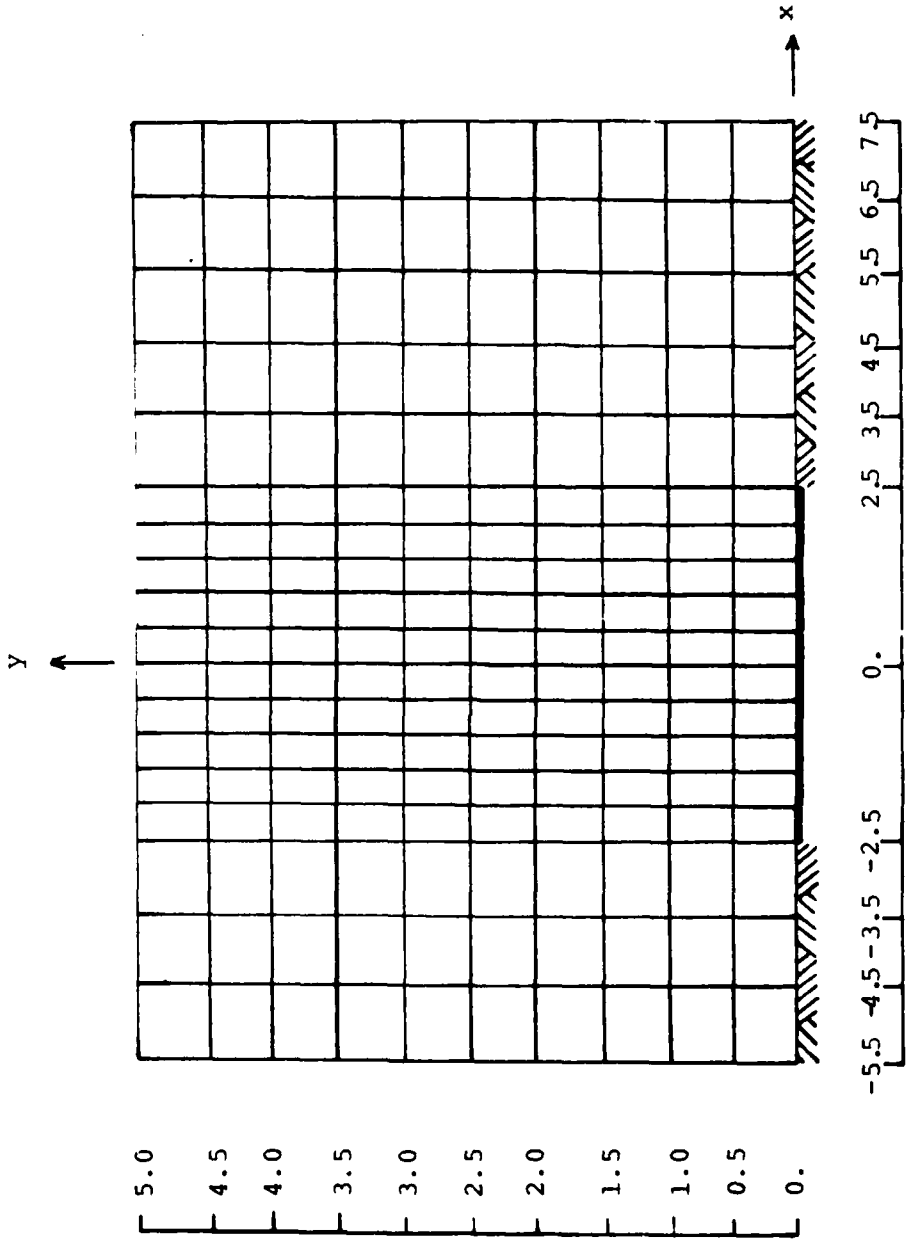

Fig. 5.6. Mesh for membrane and fluid.

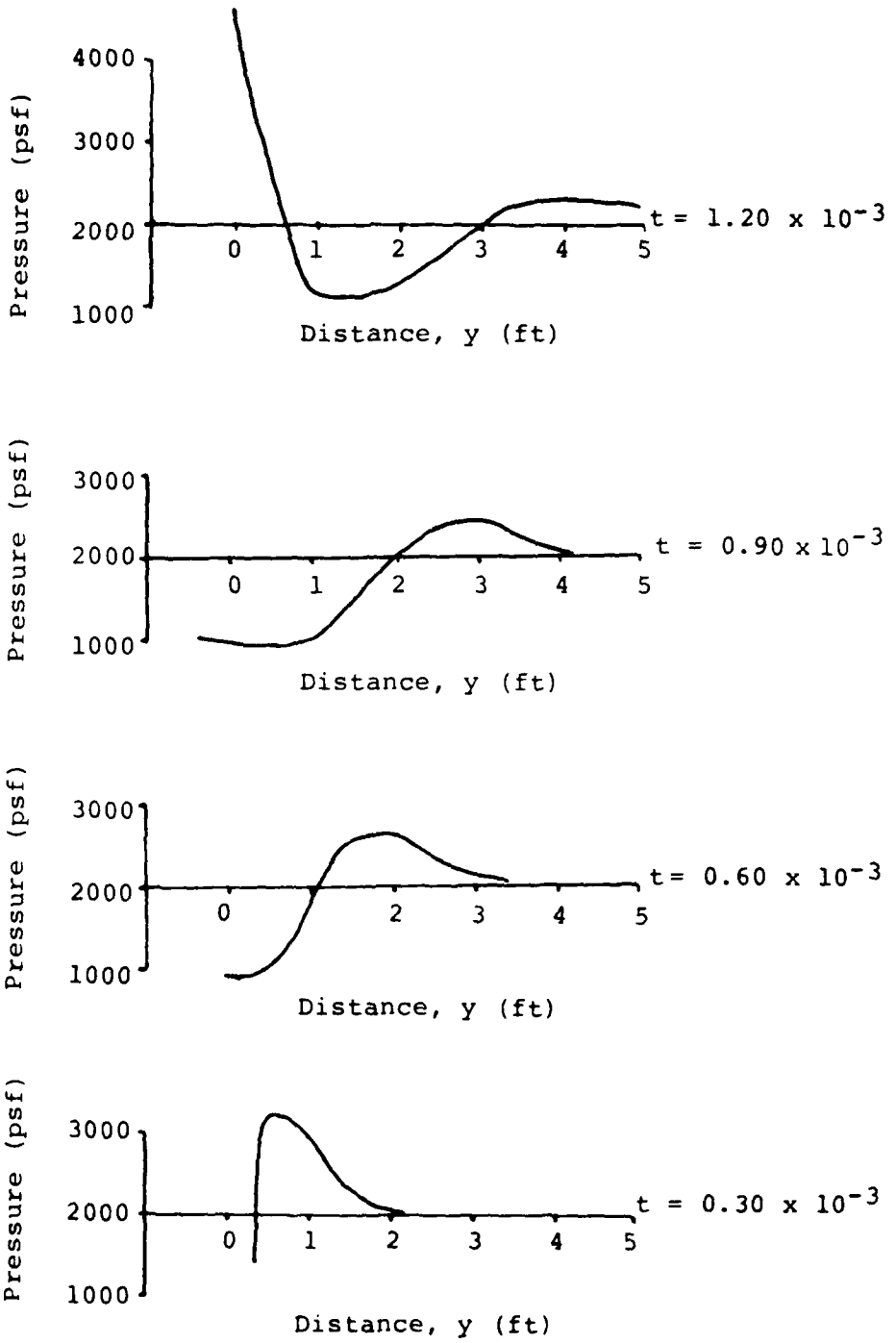

Fig. 5.7. Pressure at x = 0.

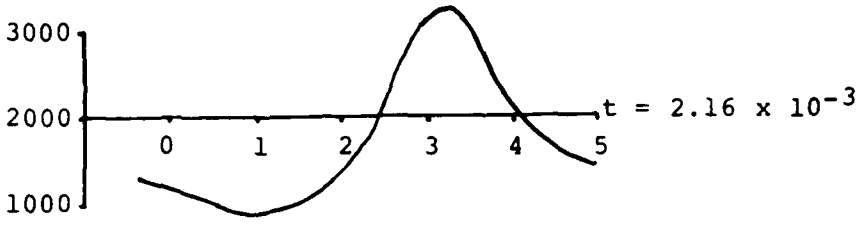

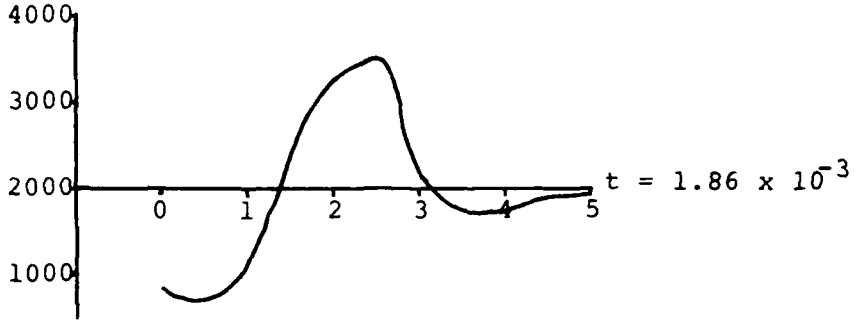

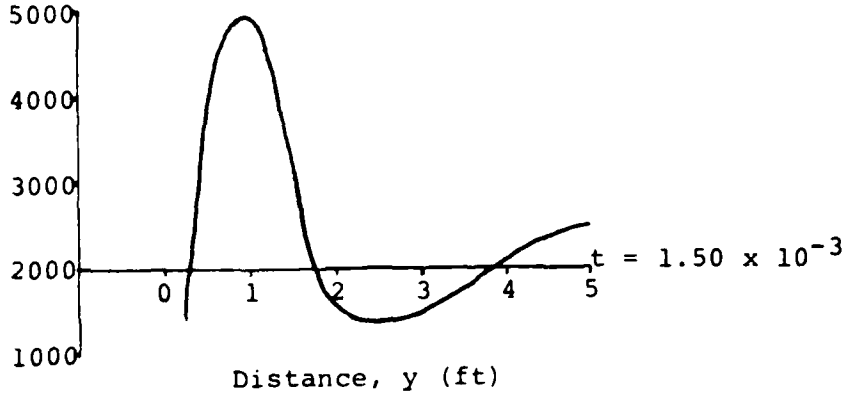

Fig. 5.7. Pressure at x = 0 (continued).

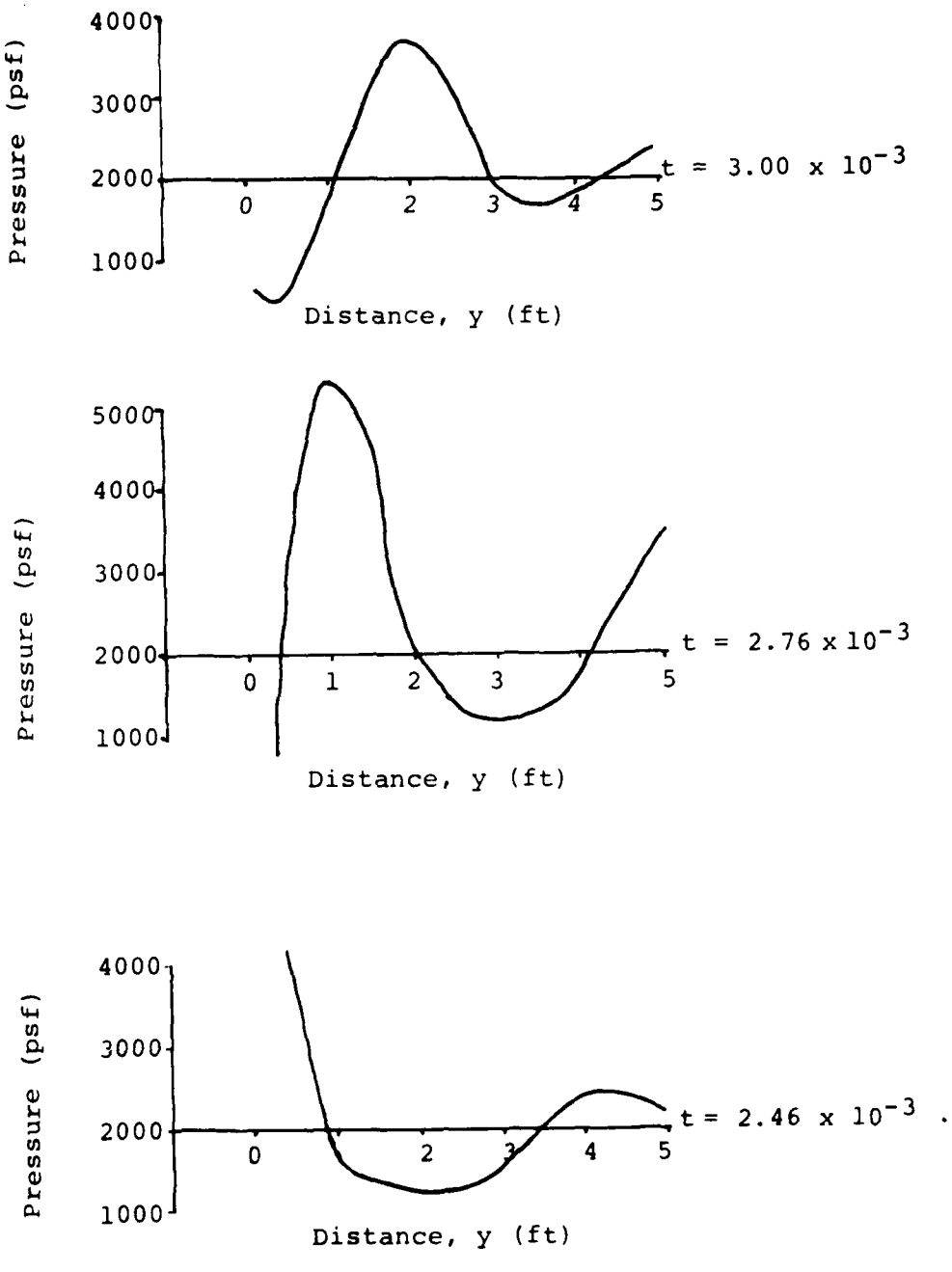

Fig. 5.7. Pressure at x = 0 (continued).

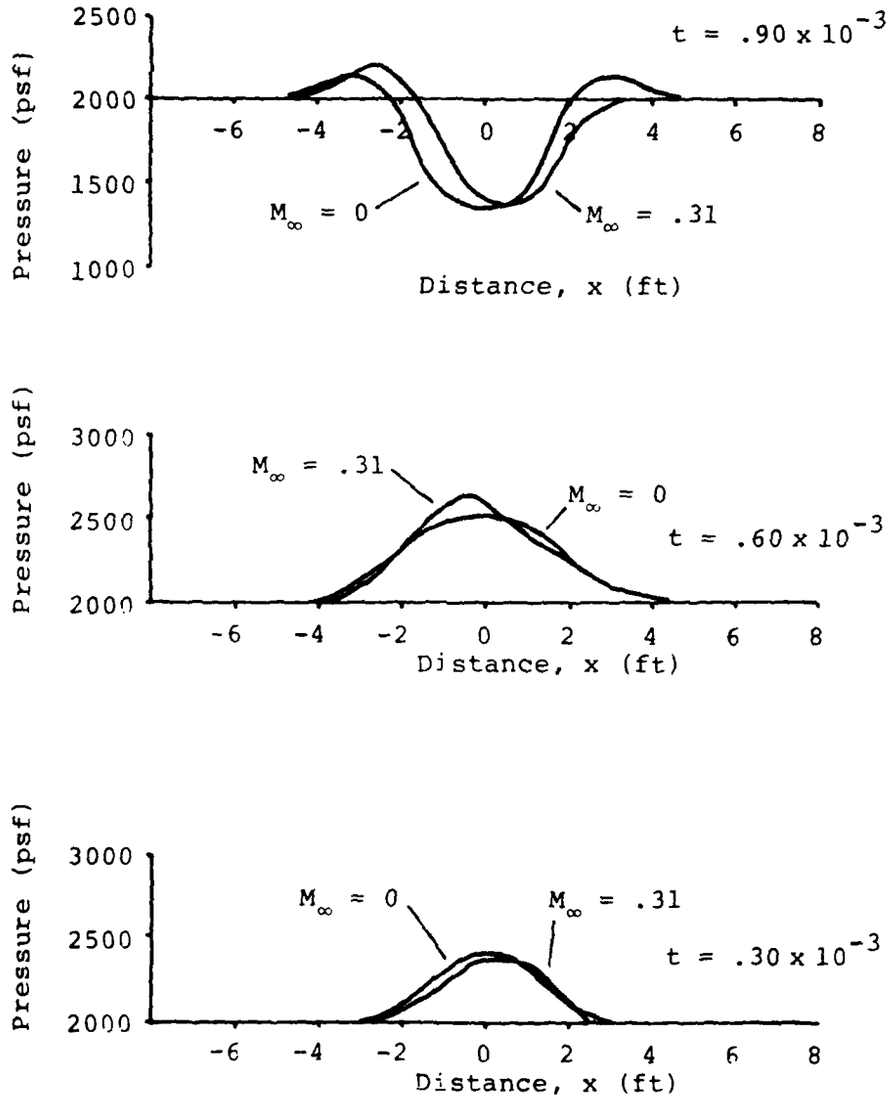

Fig. 5.8a. Pressure at y = 1.5.

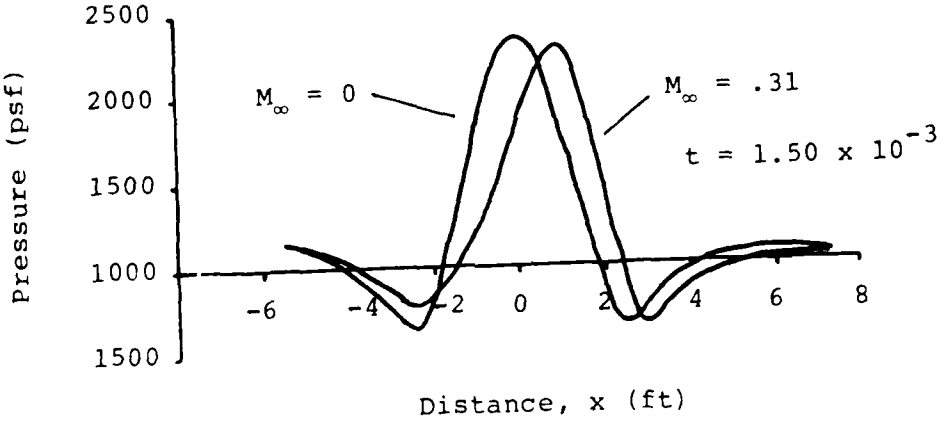

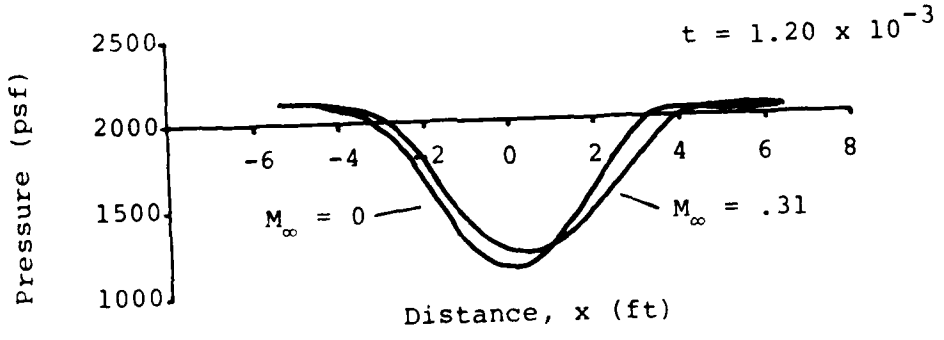

Fig. 5.8a. Pressure at y = 1.5 (continued).

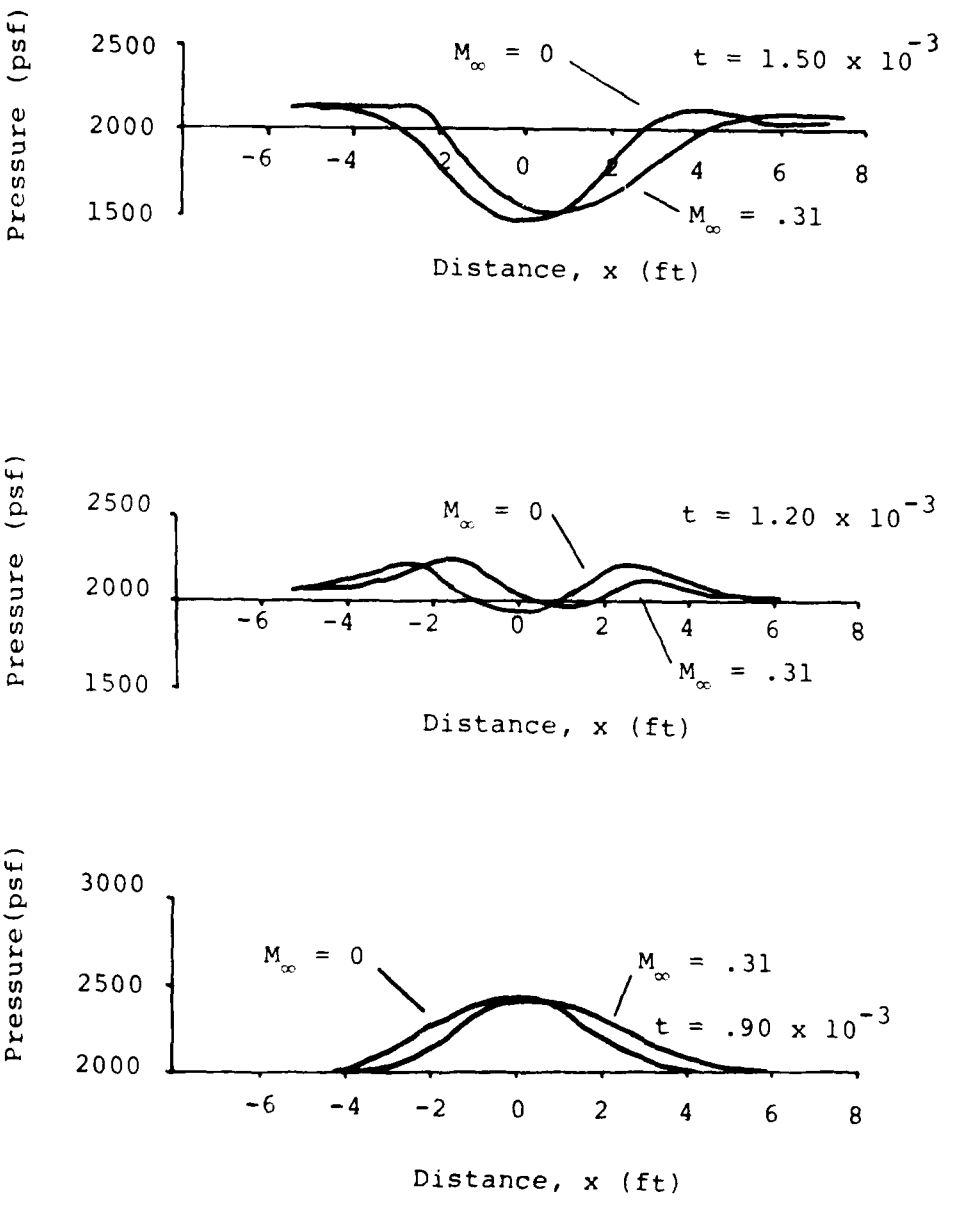

Fig. 5.8b. Pressure at y = 3.0

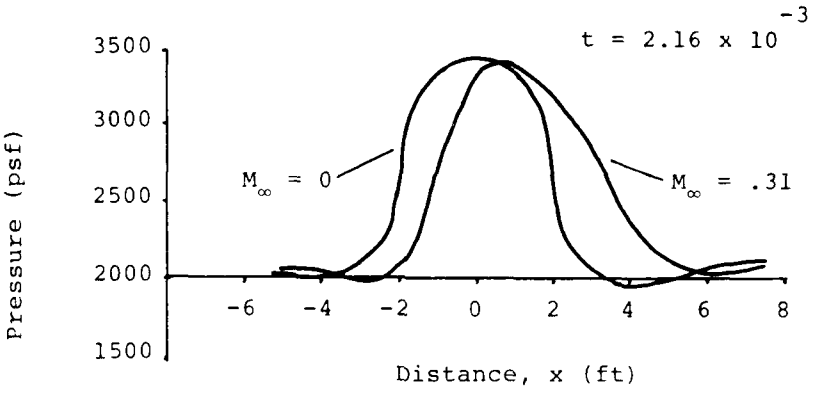

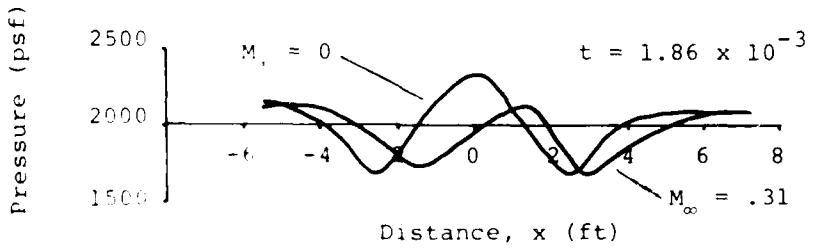

Fig. 5.8b. Pressure at y = 3.0 (continued).

AD-A106 286 AIR FORCE INST OF TECH WRIGHT-PATTERSON AFB OH F/G 20/4
FINITE ELEMENT METHOD IN TRANSIENT AEROELASTIC PROBLEM.(U)
1979 H C BRIGGS
UNCLASSIFIED AFIT-CI-79-2560 NL

END
DATE FILMED
11-81
DTIC

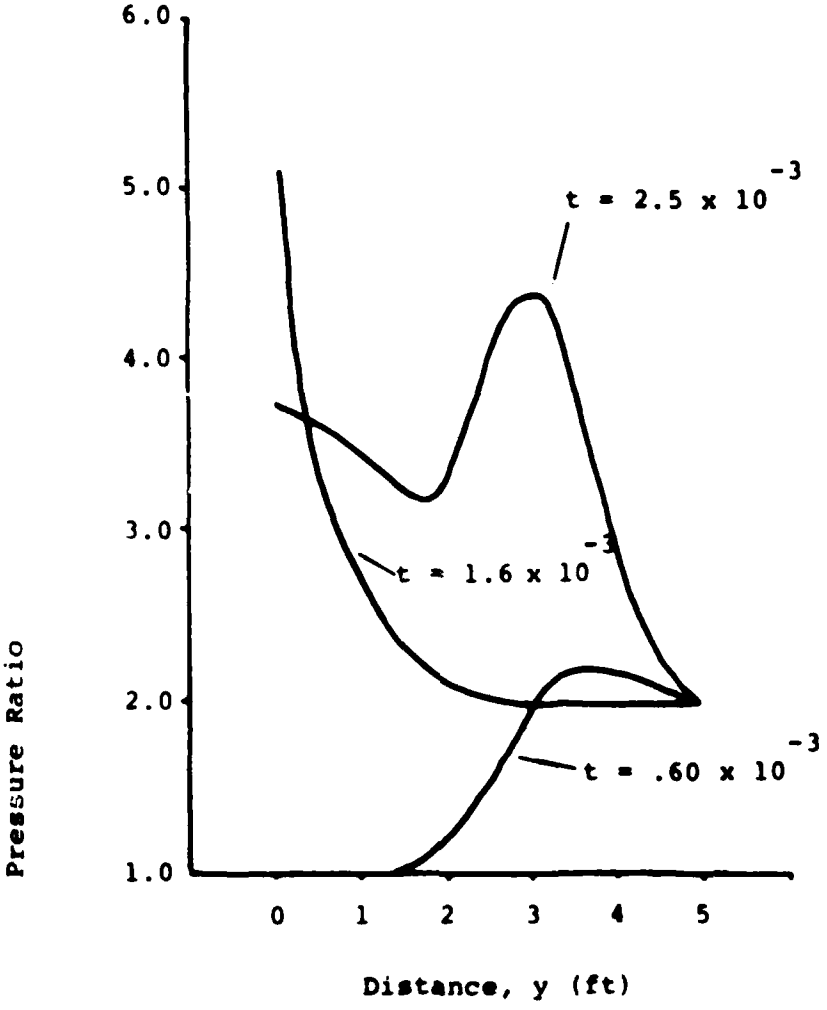

Fig. 5.9. Pressure at x = 0.

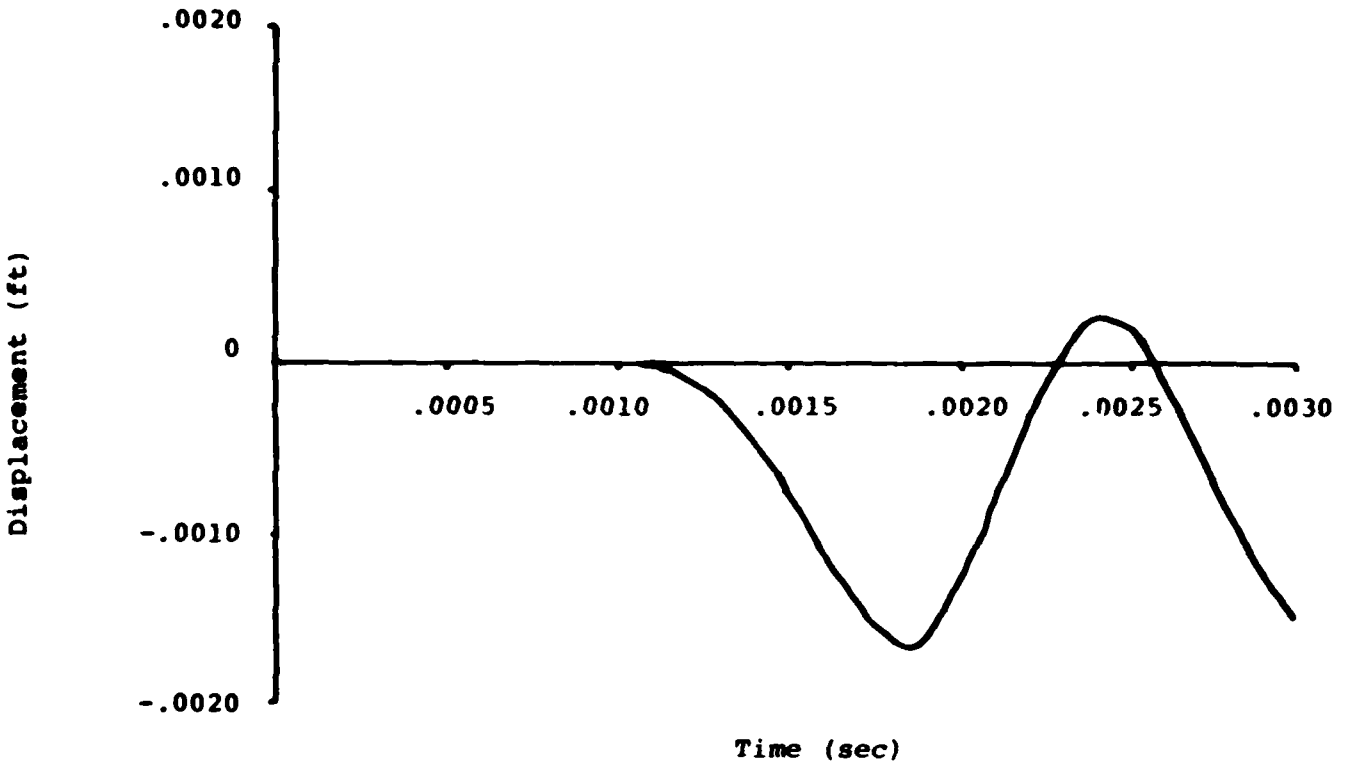

Fig. 5.10. Membrane displacement.

LIST OF TABLES

	$\beta = 1.0 \times \text{sign}(v_t)$			$\beta = 0$		
θ	v_r	v_t	p	v_r	v_t	p
0.0	384.9	0.0	2733	307.8	0.0	2481
11.5	235.2	3.9	2251	307.5	1.2	2479
22.5	374.0	-0.2	2700	307.5	0.3	2480
33.5	235.8	-1.9	2254	308.2	-0.5	2483
45.0	377.3	0.0	2709	308.2	0.0	2483
56.5	235.8	1.9	2254	308.4	0.5	2483
67.5	374.0	0.2	2701	307.5	-0.3	2480
78.5	234.9	-3.8	2251	307.5	-1.2	2479
90.0	384.9	0.0	2733	307.8	0.0	2481

Note: p_0 = 1700 psf, a_0 = 1000 fps and Δr = .125 ft.

Table 5.1. Cylindrical wave solution at t = .003 sec, r = 3.0 ft, with and without cross wind weighting.

x	u_y	v_x		p	
		$M_\infty = .31$	$M_\infty = 0.$	$M_\infty = .31$	$M_\infty = 0.$
-5.5	0.	1000	0.	2000	2001
-4.5	0.	984	-9.7	2001	2001
-3.5	0.	948	-24.7	2120	2083
-2.5	0.	135	-1103	2242	2061
-2.0	.1209	476	-463	2605	2192
-1.5	.2305	648	-366	2906	2448
-1.0	.3179	886	-178	2540	2218
-0.5	.3744	1050	-53.4	1830	1724
0.0	.3939	1120	0.	1424	1435
0.5	.3744	1165	53.4	1607	1724
1.0	.3180	1252	178	1944	2218
1.5	.2305	1385	366	2071	2448
2.0	.1209	1394	463	1859	2192
2.5	0.	1936	1103	1999	2061
3.5	0.	1106	24.7	2041	2083
4.5	0.	1005	9.8	2009	2001
5.5	0.	1001	0.	2000	2001
6.5	0.	1000	0.	2000	2000
7.5	0.	1000	0.	2000	2000

Note: p_0 = 2000 psf and a_0 = 3200 fps.

Table 5.2. Fluid velocity and pressure on membrane at $t = .30 \times 10^{-3}$.

Time $\times 10^2$ (sec)	Displacement Finite Element $\times 10^3$ (ft)	Displacement Modal Expansion $\times 10^3$ (ft)
.132	-.258	-.263
.144	-.573	-.601
.156	-.993	-1.08
.168	-1.40	-1.58
.180	-1.62	-1.88
.192	-1.56	-1.81
.204	-1.17	-1.34
.216	-.599	-.633
.228	-.058	.030
.240	.237	.385
.252	.184	.304
.264	-.183	-.159
.276	-.728	-.814
.288	-1.24	-1.42
.300	-1.54	-1.76

Table 5.3. Membrane response to incident pressure wave.

REFERENCES

Argyris, J.H. and Mareczek, G. (1973). "Potential Flow Analysis by Finite Elements," Ing-Arch., 42, pp. 1-25.

Atkatsh, R., Baron, M.L. and Bieniek, M.P. (1978). "Dynamic Elasto-Plastic Response of Submerged Shells," Technical Report, Weidlinger Associates, New York, N.Y.

Baker, A.J. (1974). "A Finite Element Algorithm for Navier Stokes Equations," NASA CR-2391, June, 1974.

Carey, G. F. (1975). "A Dual Perturbation Expansion and Variational Solution for Compressible Flows using Finite Elements," from International Conference on the Finite Element Method in Flow Analysis, University College of Wales, 1974, edited by R.H. Gallagher, J. Wiley and Sons.

Christie, I., Griffiths, D.F., Mitchell, A.R. and Zienkiewicz, O.C. (1976). "Finite Element Method for Second Order Differential Equations with Significant First Derivatives," Int. J. for Num. Meth. Eng., Vol. 10, pp. 1389-1396.

Chung, T.J. (1978). Finite Element Analysis in Fluid Dynamics, McGraw-Hill.

Delleur, J. and Sooky, A. (1961). "Variational Methods in Fluid Dynamics, Proc. Am. Soc. Civ. Eng., 87, EM6, pp. 57-77.

DiMaggio, F.L., Bleich, H.H. and McCormick, J.M. (1978). "Dynamic Response of a Containment Vessel to Fluid Pressure Pulses," Computers and Structures, Vol. 8, pp. 31-39.

Dowell, E.H. (1966). "Nonlinear Oscillations of a Fluttering Plate," Pt. I, AIAA J. Vol. 4, July 1966, pp. 1267-1275; Pt. II, AIAA J. Vol. 5, Oct. 1967, pp. 1856-1862.

Dowell, E.H. (1970). "Panel Flutter: A Review of the Aeroelastic Stability of Plates and Shells," AIAA J. Vol. 8, Mar. 1970, pp. 385-399.

Dusto, A.R., Epton, M.A. and Johnson, F.T. (1978). "Advanced Panel Type Influence Coefficient Methods Applied to Unsteady Three Dimensional Potential Flows," AIAA, Paper No. 78-229.

Evensen, D.A. and Olson, M.D. (1968). "Circumferentially Traveling Wave Flutter of a Circular Cylindrical Shell," AIAA J. Vol. 6, No. 8, Aug. 1968, pp. 1522-1527.

Everstine, G.C., Schroeder, E.A. and Marcus, M.S. (1975). "The Dynamic Analysis of Submerged Structures," NASTRAN: User's Experiences, NASA TM X-3278, Sept. 1975.

Everstine, G.C. (1976). "A NASTRAN Implementation of the Doubly Asymptotic Approximation for Underwater Shock Response," NASTRAN: User's Experiences, NASA TM X-3428, Oct. 1976.

Finlayson, B.A. (1972). The Method of Weighted Residuals and Variational Principles, Academic Press.

Geers, T.L. (1975). "Transient Response Analysis of Submerged Structures," from Finite Element Analysis of Transient Nonlinear Structural Behavior, edited by T. Belytschko, et al., ASME, AMD, Vol. 14.

Giesing, J.P., Kalman, T.P. and Rodden, W.P. (1972). "Subsonic Steady and Oscillatory Aerodynamics for Multiple Interfering Wings and Bodies," J. Aircraft, Oct. 1972, pp. 693-702.

Gotta, E.F.F. and van de Vooren, A.I. (1972). "Calculation of Potential Flow about Aerofoils using Approximation by Splines," from Contributions to the Theory of Aircraft Structures, Delft University Press.

Heinrich, J.C., Huyakorn, P.S., Mitchell, A.R. and Zienkiewicz, O.C. (1977). "An 'Upwind' Finite Element Scheme for Two-Dimensional Convective Transport Equation," Int. J. for Num. Meth. Eng., Vol. 11, pp. 131-143.

Jacobson, M.J., Yamane, J.R. and Brass, J. (1977). "Structural Response for Detonating High Explosive Projectiles," J. Aircraft, Vol. 14, No. 8, pp. 816-821.

Jordan, P.F. (1978). "Reliable Lifting Surface Solutions for Unsteady Flow," AIAA Paper No. 78-228.

Kornecki, A., Dowell, E.H. and O'Brien, J. (1976) "On the Aeroelastic Instability of Two-Dimensional Panels in Uniform Incompressible Flow," J. Sound and Vibration, 47(2), pp. 163-178.

Liepman, H.W. and Roshko, A. (1957). Elements of Gasdynamics, J. Wiley and Sons.

Morino, L. (1973). "A General Theory of Unsteady Compressible Potential Aerodynamics," NASA TR-73-01, Jan. 1973.

Nakamura, S. (1977). Computational Methods in Engineering and Science, J. Wiley and Sons.

Nickell, R.E. and Sackman, J.L. (1968). "Variational Principles for Linear Coupled Thermoelasticity," Q. Appl. Math., 26, pp. 11-26.

Nikolakopoulou, G. and DiMaggio, F. (1978). "Dynamic Elastic-Plastic Response of a Containment Vessel to Fluid Pressure Pulses," Columbia University, Dept. of Civil Engineering and Engineering Mechanics Report, Feb. 1978.

Norrie, D.H. and de Vries, G. (1973). The Finite Element Method, Academic Press.

Oden, J.T. and Somogyi, D. (1969). "Finite Element Applications in Fluid Dynamics," J. Eng. Mech. Div. Proc. ASCE, 95, No. EM 3, pp. 821-826.

Olson, M.D. (1970). "Some Flutter Solutions using Finite Elements," AIAA J. Vol. 8, No. 4, Apr. 1970, pp. 747-752.

Parkinson, G.V. and Jandali, T. (1970). "A Wake Source Model for Bluff Body Potential Flow," J. Fluid Mech., Vol. 40, pp. 577-594.

Pittman, J.L. and Dillon, J.L. (1977). "Vortex Lattice Prediction of Subsonic Aerodynamics of Hypersonic Vehicle Concepts," J. Aircraft, Vol. 14, No. 10, pp. 1017, 1018.

Ranlet, D., DiMaggio, F.L., Bleich, H.H. and Baron, M.L. (1977). "Elastic Response of Submerged Shells with Internally Attached Structures to Shock Loading," Computers and Structures, Vol. 7, pp. 355-364.

Rodden, W.P., Giesing, J.P. and Kalman, T. P. (1970). "New Developments and Applications of the Subsonic Doublet Lattice Method for Non-Planar Configurations," AGARD CP-80-71, Nov. 1970.

Rudinger, G. (1969). Nonsteady Duct Flow, Dover Publishers.

Serrin, J. (1959). "Handbuch der Physik," Vol. 8/1, Springer-Verlag, Berlin.

Steele, N.C. and Barrett, K.E. (1978). "A 2nd Order Numerical Method for Laminar Flow at Moderate to High Reynolds Numbers: Entrance Flow in a Duct." Int. J. Num. Meth. Eng. Vol. 12, p. 405-414.

Tözeren, H. and Skalak, R. (1978). "The Steady Flow of Closely Fitting Incompressible Elastic Spheres in a Tube," J. Fluid Mech., Vol. 87, Pt. 1, pp. 1-16.

Tuann, S.Y. and Olson, M.D. (1976). "A Study of Various Finite Element Solution Methods for Navier Stokes Equations," Structures Report No. 14, Dept. of Civil Engineering, UBC, Vancouver, B.C., Canada.

Wang, P.K.C.(1966). "Stability Analysis of Elastic and Aeroelastic Systems via Lyapunov's Direct Method," J. Franklin Inst., 28(1), pp. 51-72.

Zarda, P.R. (1976). "A Finite Element Analytical Method for Modeling a Structure in an Infinite Fluid," NASTRAN User's Experiences, NASA TM X-3278, Oct. 1976.

Zarda, P.R., Chien, S. and Skalak, R. (1977). "Interaction of Viscous Incompressible Fluid with an Elastic Body," from Computational Methods for Fluid-Structure Interaction Problems, edited by T. Belytschko and T.L. Geers, ASME, AMD, Vol. 26.

Zienkiewicz, O.C. (1977). The Finite Element Method, Third Edition, McGraw-Hill.

Zienkiewicz, O.C., Kelly, D.W. and Bettess, P. (1977). "The Coupling of the Finite Element Method and Boundary Solution Procedures," Int. J. for Num. Meth. Eng., Vol. 11, No. 2, pp. 355-375.

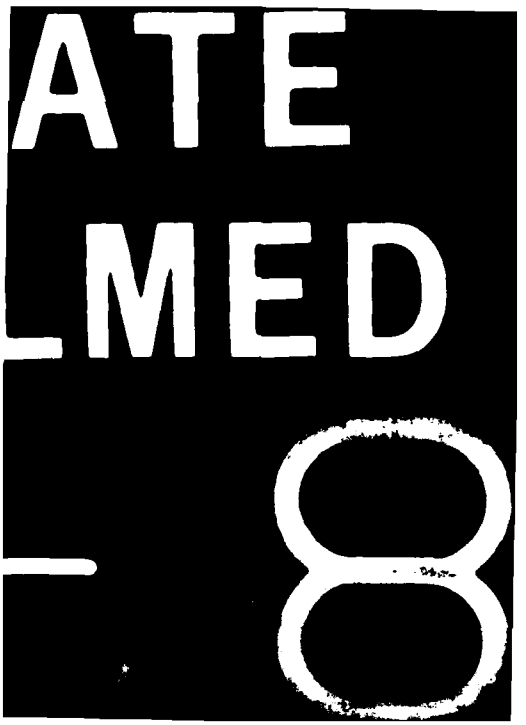
ATE
LMED
8